THE PENNSYLVANIA STATE UNIVERSITY
SCHREYER HONORS COLLEGE

DEPARTMENT OF CHEMISTRY

Tracking of Progressing Human DNA Polymerase Holoenzymes Reveals Distributions of DNA Lesion Bypass Activities

JOSEPH CARDINA
SPRING 2023

A thesis
submitted in partial fulfillment
of the requirements
for a baccalaureate degree
in Chemistry
with honors in Chemistry

Reviewed and approved* by the following:

Mark Hedglin
Assistant Professor of Chemistry
Thesis Supervisor

Lauren Zarzar
Associate Professor of Chemistry
Honors Adviser

* Electronic approvals are on file.

ABSTRACT

In lagging strand DNA synthesis, DNA polymerase δ (pol δ) holoenzymes composed of pol δ and the proliferating cell nuclear antigen (PCNA) sliding clamp perform high fidelity DNA synthesis with little error. The pol δ holoenzyme occasionally encounters structural deformities in the native DNA sequence called DNA lesions. Upon encountering these lesions, it was previously believed that pol δ would stall on the DNA template at some point before the lesion launching a DNA damage tolerance (DDT) pathway to replicate the lesion and remaining DNA before allowing pol δ to resume its typical high fidelity DNA synthesis. Recent literature within the past 20 years or so has challenged this perspective by showing human pol δ can replicate various DNA lesions. These studies have questioned the role that DDT plays in lagging strand DNA synthesis upon encounter of a DNA lesion, thus providing a need for further analysis. As a result, we aimed to quantitatively characterize the encounters of pol δ with several biologically relevant DNA lesions at physiological conditions. Our results show that pol δ supports dNTP incorporation while inserting across from, extending from, and elongating past several different DNA lesions, and the exact extent of these values is dependent on the exonuclease activity of pol δ and the identity of the lesion itself. We also found that of the pol δ that dissociates upon encountering the lesion, the dissociation events are unevenly distributed around the lesion with different distributions depending on the lesion. Our findings show that lagging strand DNA synthesis is more complex than previously thought while advancing our understanding of the role of DDT in lagging strand DNA synthesis.

TABLE OF CONTENTS

LIST OF FIGURES

ACKNOWLEDGEMENTS

I first would like to thank my mother and father, Jennifer, and Andrew Cardina for raising me into the man I am today. I could not fathom what life would be like without them and their endless support in whatever interests me. I would also like to thank my brothers Robbie, Michael, and Jonny. Family is something I prioritize and value greatly in my life. I would do anything for them, as I know they would do the same for me.

I would next like to thank my middle school science teacher, Kerry Mulvihill. Without her simple challenge of my motivation, I am not sure I would be in the position I am in today.

A massive thank you goes out to professor of Chemistry, Dr. Mark Hedglin. Mark first took me under his wing the spring of my sophomore year where he encouraged me to apply for the Benkovic Summer Research Award. Fast forward two years later and here I am etching in the final touches on my undergraduate research experience. Mark has taught me many things over my undergrad including lab techniques, writing skills, and life skills. Mark and I instantly bonded over Bruce Springsteen, although he has never heard the song “New York City Serenade”. Mark is as good of a teacher as he is a mentor, where I had the privilege of taking two of his courses with those being CHEM 112 and CHEM 597. It was through CHEM 112 and BIOL 230W that I found interest in Mark’s lab. Mark has always been encouraging yet challenging me to become the best researcher and person that I can be. Mark has been exceptionally flexible throughout the last two years providing me with guidance, recommendation letters, and countless opportunities. A special thanks also goes to Sam, Jess, Kara, and Rachel for their advice and good memories created in the lab. As I move forward into my next chapter, I will always be grateful for the time I got to spend in the Hedglin Lab.

Thank you to both my chemistry advisor, Linlin Jensen, my honors advisor, Dr. Lauren Zarzar, and my former athletic advisor, Lori O'Donnell. Each of them were very patient and understanding of my many scheduling issues throughout my undergraduate experience balancing classes and a varsity athletic schedule.

I would like to thank my honors professors Dr. Tei-Hui Kao, Dr. Song Tan, and Dr. Mark Hedglin who were my professors for BMB 402H, BMB 401H, AND CHEM 597, respectively. Each of their classes were extremely challenging yet rewarding in their own ways. I feel that I have elevated as a learner in each of their classes and from them as professors.

Lastly, thank you to the Schreyer Honors College. Being apart of this college for my last two years have provided me with excellent opportunities, relationships with friends and faculty, and development as a learner. I will always remember these experiences and the opportunity to create a senior thesis at Penn State University.

Funding to support research includes National Institute of General Medical Sciences of the National Institutes of Health [1 R35 GM147238-01 to M.H.]; Stephen and Patricia Benkovic Summer Research Award in Chemistry. Eberly College of Science Undergraduate Research Award. Funding for open access charge: National Institute of General Medical Sciences (NIGMS) of the National Institutes of Health (NIH). Results may not necessarily represent the views of these foundations.

Chapter 1

Background of DNA Replication

In the human cell cycle, there are several phases, G_0, G_1, S, G_2, and M. G_1, S, and G_2 are subcategories of interphase, and M represents mitosis, or the actual process of a parent cell dividing into two daughter cells. G_1 and G_2 are referred to as growth phases where the cell is growing and preparing for a future phase which are S phase and mitosis, respectively. Our genetic information, i.e. genome, is encoded in template strands of deoxyribonucleic acid (DNA) that base pair in an antiparallel orientation forming a double helical structure. The human DNA genome is replicated in a semi-conservative manner during S phase of the cell cycle so that each daughter cell receives a copy during cell division. This, along with many other regulated checkpoints, must be completed before a cell can enter mitosis and divide[1]. One of the keys to ensuring proper cell function and gene expression is proper DNA replication. Moreover, each template base whether it be adenine, guanine, thymine, or cytosine must be accurately copied in the exact order in which they are placed. A single insertion, deletion, substitution, or other disruption in the DNA sequence could potentially cause major changes in gene expression or protein formation. Said disruptions, if not fixed, have the potential to cause permanent mutagenic and potentially metastatic events.

To ensure the complete and accurate replication of DNA, an assortment of replicative enzymes are carefully used, with the primary enzymes being DNA polymerases (pols). Which synthesize and replicate DNA in the 5'→3' direction. DNA synthesis by pols is important in many cellular processes, including replication, repair, recombination, and lesion bypass. Until

the 1970's, it was thought that DNA was replicated solely by pol α and there were only three known pols, due to unadvanced research on the subject area. It was then discovered in the following decades that pol α was one of three primary replicative proteins; pol α, pol ε, and pol δ[2]. Pol α inserts ribonucleic acid (RNA) primers on a template DNA strand and may replicate up to the first 30 bases of DNA on both the leading and lagging strands. The work done by pol α is the first replication in DNA synthesis after helicase unwinding of double stranded DNA (dsDNA)[3]. Such work is essential as both nucleotide extension polymerases require a primer to properly function. Pol ε and pol δ extend the primers placed by pol α on the leading and lagging strands, respectively[4,5]. The three primary human, and eukaryotic, replicative pols are all part of the B family polymerases[6]. The pol used in all experiments discussed in this paper is the human lagging strand DNA polymerase, pol δ.

Pol δ was discovered and isolated by an investigative team at University of Miami, Florida studying rabbit bone marrow erythroid cells, calf thymus, and human placental tissues[7-18]. Their studies also concluded that pol δ contained a 125kDa catalytic subunit that contained both polymerase and exonuclease active sites. Once it was confirmed that pol δ was a separate polymerase from pol α via molecular cloning of the 125 kDa subunit, it was confirmed that pol δ was the first polymerase of its kind with exonuclease activity, which is also referred to as proofreading[19-21]. Recent literature has confirmed that pol δ contains four subunits, p50, p66, p12, and the catalytic subunit p125 which contains active sites for DNA polymerase and 3'→5' exonuclease activities which agrees with preliminary studies on this subunit[22]. The cysteine rich region on the C-terminus of the p125 catalytic subunit is where the p50 subunit attaches to. The p50 and p66 subunits are tightly bound. The p125 subunit resembles a right hand[27], where the palm, fingers, and thumb of the hand form a pocket where nucleotide incorporation takes place.

The thumb is used to hold the DNA duplex and helps chaperone the primer strand as it travels to the exonuclease domain for proofreading[27,28]. In summary, Pol δ is a heterotetrametric enzyme containing12 kDa (POLD1), 50kDa (POLD2), 66kDa (POLD3), and 125 kDa (POLD4) subunits[22].

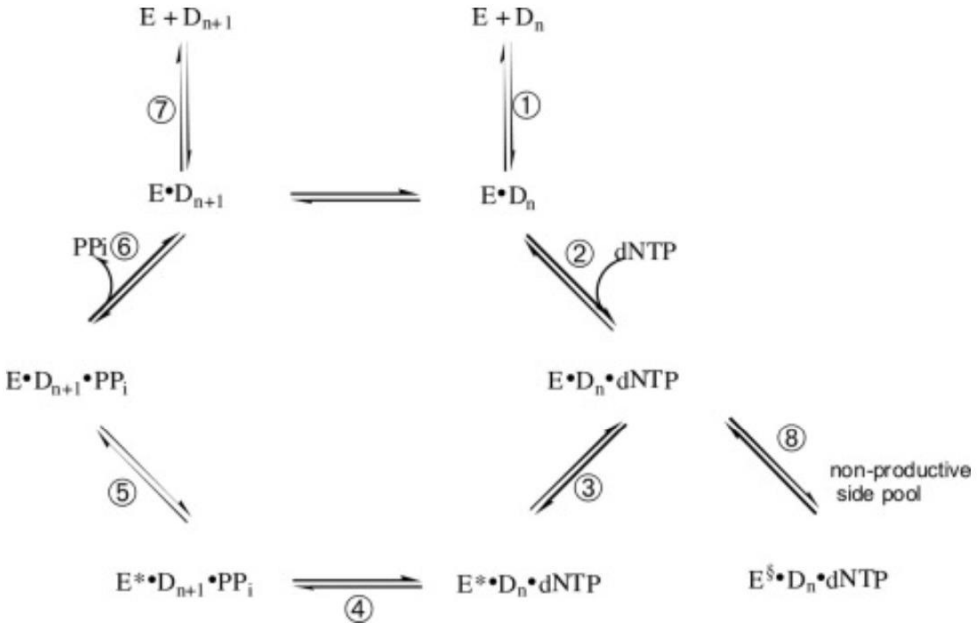

Figure 1. Minimal kinetic mechanism of pol δ facilitating DNA replication[72].

Eukaryotic pol δ has a complex kinetic mechanism due to its binding of multiple substrates and multiple catalytic paths that can be taken. The simplified catalytic mechanism in Figure 1, above, involves a combination of reversible or irreversible first and second order elementary reactions. This simplified mechanism focuses on binding, chemistry, and conformational change steps. Pol δ is indicated by E, Dn indicates a DNA substrate. E^{*} represents a conformational change in pol δ. $E^{§}$ represents a conformationally inactive form of pol δ. D_{n+1} indicates extension of DNA by one nucleotide in length. PP_i, seen in steps 5 and 6, shows pyrophosphate. Pol δ begins by binding to DNA in step 1. Next, the pol δ-DNA duplex binds a dNTP. Following this, pol δ undergoes one of two conformational changes with one

being preparation for catalysis and the other inactivating pol δ. If step 3 occurs, then pol δ is prepared to perform the chemistry step in this mechanism which is the polymerization of one nucleotide to the existing DNA strand. Next, pol δ returns to its original conformation in step 5, and PPi is released in step 6. The pol δ-DNA duplex after step 6 is identical to the pol δ-DNA duplex shown after step 1. From here, pol δ may either repeat and perform another turnover, or it can dissociate from the DNA complex, as seen in figure 1. The complex mechanism of pol δ involves numerous reactions and moving parts that must be kinetically completed very fast to ensure normal cell proliferation during S phase.

Pol δ alone is a very inefficient DNA pol due to its low attraction to primer/template (P/T) DNA[23]. Due to this, pol δ is aided by other replication proteins and factors to improve stability and efficiency of replication. With millions of nucleotides to replicate in the human genome, pol δ must replicate at very fast rates to keep up with cellular growth rates. To do this, pol δ attaches to a processivity sliding clamp, proliferating cell nuclear antigen (PCNA), forming a holoenzyme. As a holoenzyme, pol δ has dramatically increased nucleotide incorporative efficiency and processivities[23]. PCNA is believed to interact with the p50 and p125 subunits of pol δ[24,25]. PCNA is a closed ring/toroid that is opened and loaded onto P/T DNA by replication factor C (RFC), discussed later. PCNA moves freely on dsDNA[29]**.** The p12 subunit of pol δ also increases the processivity of the enzyme by up to 15-fold through PCNA interaction[26]. The dual contributions of the p12 subunit and PCNA permit a high extent of continuous replication.

For PCNA to interact with pol δ, it must be loaded onto P/T DNA by RFC. RFC contains five subunits and has varying binding affinities for P/T DNA that are dependent on the availability of ATP. Kinetic studies have shown that RFC has a high affinity for template sites that need PCNA to be loaded but have low affinities for template sites that contain pol δ to not

interfere with pol δ enzyme catalysis[30]. ATP hydrolysis by RFC is dependent on DNA presence, which creates a structural shift in the RFC complex that allows for subsequent ATP hydrolysis[31]. The binding of ATP to RFC promotes favorable interactions between site specific RFC and PCNA domains. Next, the PCNA/RFC complex recognizes the P/T junction and adopts a structural conformation that fits the double helical geometry of the P/T DNA. Once loaded, ATP is hydrolyzed and RFC switches to its low affinity DNA binding state. RFC then dissociates from PCNA, leaving PCNA behind on the P/T DNA to interact with pol δ[31]. ATP catalyzed site-specific loading of PCNA onto P/T DNA by RFC is an essential enzymatic process that heavily increases pol δ fidelity and processivity via formation of the pol δ holoenzyme.

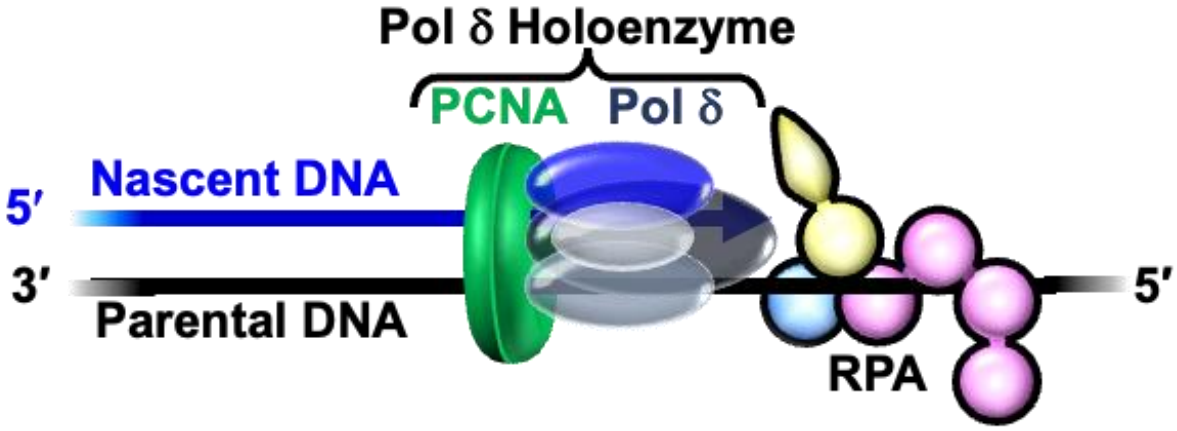

Figure 2. General schematic of pol δ complex during lagging strand DNA replication.

Single strand DNA templates that are exposed during DNA replication by DNA helicase-mediated unwinding of the parental DNA duplex are immediately engaged by single stranded binding proteins (SSBs). In eukaryotes, the most prevalent SSB is replication protein A (RPA), shown in figure 2, whose primary function is to encapsulate ssDNA to prevent the formation of harmful secondary structures within the ssDNA and to prevent degradation by cellular nucleases. RPA also plays a more enhanced role in DNA repair and recombination pathways[32,33]. Eukaryotic RPA, including human RPA, is a heterotrimeric protein containing subunits of 70,

32, and 14 kDa[34,35]. RPA becomes phosphorylated by DNA-dependent protein kinase upon binding to ssDNA during synthesis and after DNA damage. RPA phosphorylation could also play an essential role in DNA metabolism[32]. RPA location in the cell varies with respect to the phase of cell cycle the cell is presently in. During S phase, RPA is found to localize around replication centers inside the nucleus[36-39]. RPA in general plays an essential role in DNA replication via binding to ssDNA and preventing any harmful secondary structures from forming.

Chapter 2

Errors in DNA replication

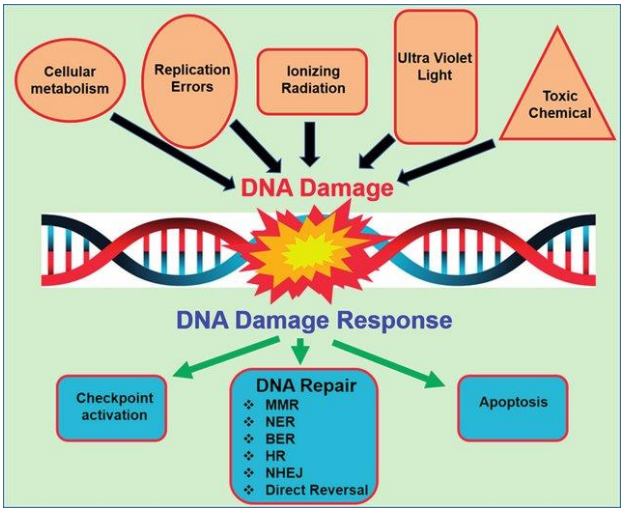

Figure 3. Schematic of DNA damage and response pathways[41].

Human DNA cells are believed to have mutation frequencies of 1 per 1 billion base pairs[40]. This rate is very low, however is essentially what gives arise to all the genetic variations between humans. For a mutation to become part of the human genome, a base pair must be wrongfully replicated. Next, the incorrect inserted nucleotide must be replicated again. By doing this, two cycles of replication have occurred, and our replication repair machinery will no longer be able to detect anything that is wrong. A significant number of DNA mutations are caused by DNA lesions. Lesions are covalent modifications of native nucleotides that cause difficulty in replication due to pols inability to replicate the lesion in its active site. Seen in figure 3, DNA lesions may arise from cellular metabolism which produces reactive oxygen species as a result. DNA lesions also frequently arise from the toxins in the foods we eat. Ionizing radiation arises from harmful substances as well as toxic chemicals. Lastly, UV light causes DNA damage and can occur environmentally from the sun or chemically from tanning beds among other things.

The types of DNA damage seen in figure 3 can be grouped into two categories based on the location of which they arise. These locations are exogenous and endogenous which represent outside or inside the body, respectively.

Most endogenous DNA damage stems from DNA undergoing hydrolytic and oxidative reactions with reactive oxygen species (ROS) that persist naturally within the cell and are in fact a byproduct of cellular metabolism in the electron transport chain[42-44]. Surprisingly, ROS are beneficial in cells at low levels. They serve as cellular messengers in redox reactions within the cell by sparking defense responses to invading pathogens by the immune system[45-47]. However, ROS at higher levels can cause over 100 different oxidative lesions to native templates[48]. ROS

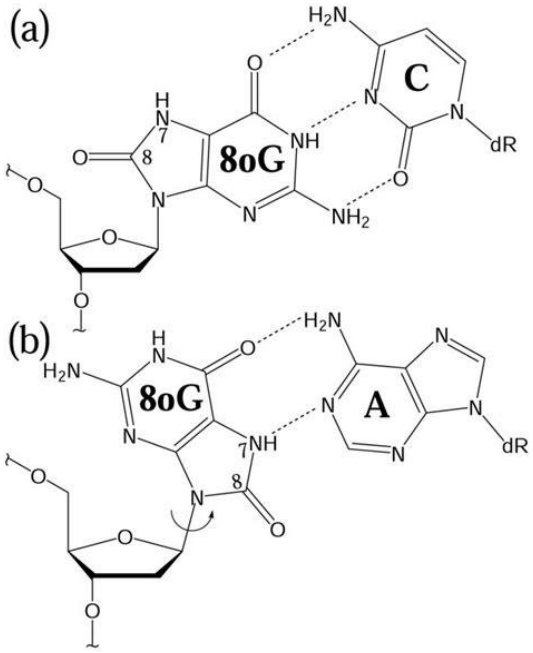

Figure 4. Syn and Anti conformations of 8-oxo-G. A) 8-oxo-G paired with correct Cytosine in syn position. B) 8-Oxo-G mispaired with Adenine in anti-conformation[54].

exist in many variations, but always involve oxygen with a free radical attached to it. The most common examples of ROS are superoxide radicals ($*O_2^-$), hydrogen peroxide (H_2O_2), and the hydroxyl radical (*OH)[49]. The hydroxyl radical is the most reactive of the three, commonly damaging DNA, proteins, and even lipids[50]. One of the most common oxidative lesions that

exists is the 7,8 dihydro-8-oxoguanine (8oxoG) lesion (Figure 4), which is also characterized in this paper. This lesion is formed via hydroxylation of the C-8 residue of guanine. 8-Oxo-G is known to pair incorrectly with adenine as well as correctly with guanine. As shown in figure 4a, the syn conformation of 8oxoG demonstrates a typical guanine face that will base pair with cytosine in regular fashion. However, in the anti-conformation, the 8oxoG lesion is rotated 180^{o} about the glycosidic bond and the face that is read by pol δ resembles thymine. This causes pol δ to insert incorrect Adenine across the lesion, which gives rise to many potential mutations.

Another pathway of DNA damage is methylation. S-adenosoylmethionine (SAM), is commonly used as a methyl donor in cellular reactions but can spontaneously generate methyl groups on native DNA nucleotides at alarming rates. Such rates include 4000 N7-methylguanine lesions, 600 N3-methyladenine lesions, and 10-30 O^6-methylguanine (O6meG) lesions each day in every cell in mammals[51]. Several other methylating agents exist including nitrosylated bile salts, betaine, chlorine which exist endogenously and tobacco smoke, food from our diet, and pollutants which exist exogenously[52,53]. These lesions, specifically O6meG, produce a significant structural difference and are highly mutagenic. The most common mutation produced by O6meG is G:C→A:T mutation. O^6-meG is a primary lesion used in this study. Other alkylating lesions that exist are O4-methylthymine, O4-ethylthymine, N7-methylguanine, N3-methyladenine, N3-methylthymine and N3-methylcytosine. Said lesions range in their destructiveness from none to major, depending on their structure and if they have an associated effective cleaving protein. Most methylated lesions are removed from the DNA via O6MeG methyltransferase or oxidation by an α-ketoglutarate-dependent dioxygenase AlkB homolog. These enzymes essentially reverse the DNA damage done by alkylating agents. The other removal pathway is base excision repair

(BER) where glycosylases work to fix the methylated damaged base via cleavage of the glycosidic bond connecting the deoxyribose sugar to the template base[55].

Exogenous DNA damaging agents include ionizing radiation, ultraviolet (UV) radiation, alkylating agents, aromatic amines, polycyclic aromatic hydrocarbons (PAHs), environmental toxins, environmental stresses, and other reactive electrophiles[56]. Common exogenous sources include ionizing radiation and UV radiation. Ionizing radiation stems from alpha, beta, gamma, neutron, and X-rays. Sources exist in the environment and are produced from materials ranging from rocks to medical devices. Ionizing radiation is known to damage DNA either directly or indirectly. The indirect pathway involves ionizing radiation penetrating the surrounding water to generate hydroxyl radicals which can then damage the DNA[57]. UV radiation is another common form of exogenous DNA damage. Our sun produces different wavelengths of light including visible light, IR light, and UV light. UV light from the sun is classified into three categories based on the range of wavelengths emitted: UV-C (190-290nm), UV-B (290-320nm), and UV-A (320-400nm). Given that DNA has an absorbance maximum of 260nm, UV-C is the most harmful type of UV radiation our sun emits[58]. Most of it, luckily, is absorbed by the ozone, however the rays that break through the ozone are harmful to skin. Three common lesions produced by UV-C photoproducts are cyclobutane pyrimidine dimers (CPDs), pyrimidine (6-4) pyrimidone photoproducts ((6-4) PPs), and 8oxoG. All these lesions, which arise both exogenously and endogenously can stall the pol δ holoenzyme from replicating past it. This is extremely detrimental to the cell as it leaves single stranded DNA exposed allowing for the formation of harmful secondary structures or even single or double strand breaks in the DNA.

Chapter 3

DNA Damage Repair

Luckily, mutations single handedly cannot cause cancer in humans. Rather, a myriad of events must occur in the right places at the right times for cancer to develop in the human body. In fact, to further combat metastasis, humans possess sophisticated systems including DNA repair, DNA damage tolerance, cell cycle checkpoints, cell cycle arrest, and apoptosis. All these systems collectively defend against the formation of mutations in our DNA and ultimately cancer. As discussed previously, types of DNA damage include endogenous and exogenous alkylating and oxidizing agents, among other things. DNA damages range in severity from small lesions to bulky lesions, and interstrand crosslinks. When DNA is damaged by lesions, depending on the size, two DNA repair pathways are primarily responsible for repairing the lesion. Base excision repair is typically the method of repair for damaged bases that do not significantly distort the DNA double helical structure. This typically includes small lesions resulting from oxidative, deamination, or alkylative damage such as 8oxoG lesions. Base excision repair is activated by one of many DNA glycosylases whose job it is to locate a damaged nucleotide and excise it from the DNA. To date, at least 11 different DNA glycosylases exist[61]. Nucleotide excision repair is the predominant pathway involved in the removal of bulky DNA lesions including CPDs and (6-4) PP.

DNA lesions that escape detection by the aforementioned DNA repair pathways may persist into S-phase where they are encountered by the DNA replication machinery. As pol δ holoenzyme is replicating DNA and encounters a lesion, pol δ will either replicate past the lesion, dissociate from the DNA leading to numerous unwanted events,

or Translesion DNA Synthesis can occur. Translesion DNA synthesis is an evolutionary conserved DNA damage tolerance (DDT) pathway that utilizes specialized DNA polymerases to replicate past DNA lesions. These specialized DNA polymerases are recruited to a DNA lesion upon stalling of pol δ or ε and this recruitment manifests through monoubiquitination of the resident PCNA encircling the stalled P/T DNA. TLS, DNA polymerases effectively replicate past lesions due to their active sites being much more accommodating to changes in nucleotide structure and it provides a "looser" fit than pol δ. TLS polymerases can carry out synthesis across DNA lesions with less fidelity than pol δ[64]. Once the lesion is replicated, the TLS pol may continue replicating, or pol δ may rebind to the DNA, kicking off the TLS pol, and finish remaining replication[65,66]. However, TLS polymerases do not possess exonuclease activity and are significantly more error prone than pol δ. This implies that incorrect nucleotides incorporated by TLS polymerases will become mutations in the second round of replication. Due to TLS being error prone and not having proofreading activities, the risk of cancer development when TLS is used is a concern.

Chapter 4

History of DNA Damage Tolerance

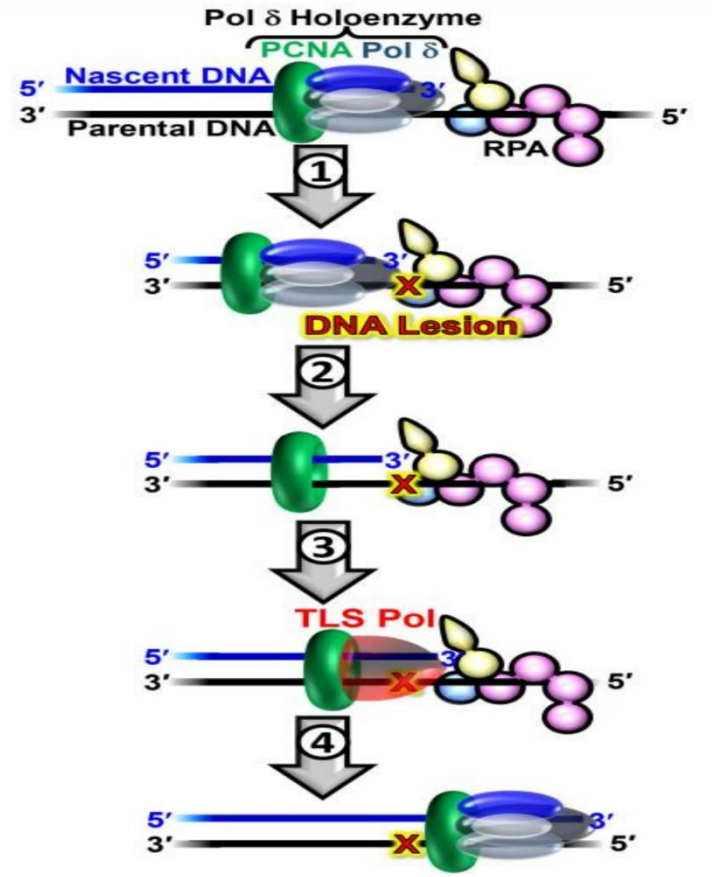

Figure 5. Previous understanding of events when pol δ encounters DNA lesions[59].

When pol δ stalls on a lagging strand template, DNA Damage Tolerance (DDT) pathways are activated. DDT resembles various mechanisms in the cell that serve to identify DNA lesions, signal the presence of the lesion, and ultimately facilitate replication of the lesion[60]. In humans, the primary DDT pathway is translesion DNA synthesis (TLS). When a replicating polymerase, like pol δ encounters a DNA lesion, it was believed that the polymerase stalls, activating TLS. Shown in figure 5, the pol δ holoenzyme , encounters a DNA lesion on a lagging strand template in part 1. In part 2, pol δ dissociates from PCNA and DNA leaving PCNA and RPA bound to the DNA. At this point, pol δ could potentially rebind to PCNA and DNA, but ultimately will not be

able to incorporate deoxyribonucleotide triphosphates (dNTPs) across from the lesion. Next, shown in part 3, the pol absent primer/template (P/T) junction will be engaged by one of several possible TLS polymerases to replicate the lesion and subsequent DNA. Replication across the lesion is referred to as insertion, replication of one nucleotide past the lesion is referred to as extension. Lastly, replication of any DNA that is more than one nucleotide downstream from the lesion is called elongation. Seen in part 4, pol δ is now re-engaged with PCNA and P/T DNA and can now replicate the remaining DNA now that the lesion is successfully bypassed. This model of TLS has been supported until recent years, where increasing numbers of studies have been published indicating the recruitment of TLS polymerases when pol δ encounters a lesion is not always the case. Here I discuss where the field sits on TLS for lagging strand DNA synthesis involving pol δ.

In 2009, the Matsumoto group concluded that pol δ could replicate past both 8oxoG lesions and apurinic/apyrimidinic (AP) sites. A is the predominant nucleotide inserted across AP sites in both the wild type and exonuclease-deficient mutants of pol δ. Both wild type and exonuclease-deficient mutants of pol δ insert correct C and incorrect A across 8oxoG lesions are relatively similar frequencies with C being inserted slightly more than A[67]. Similar conclusions regarding the bypass of 8oxoG by human pol δ were also reached in an independent study from Hubscher's group in 2012[69]. Hirota's group found in 2010 that human pol δ can replicate past cyclobutane pyrimidine dimer (CPD) and a 6-4 pyrimidone photoproduct (6-4 PP)[68]. In 2009, Loeb's team found that pol δ replicates past numerous minor to significant lesions with varying efficiencies. Specifically, pol δ replicates past 8-oxoguanine, O^6-methylguanine, O^4-methylthymine, and a synthetic abasic site, with 8oxoG and O4mT being the most successful. This agrees with previous studies on 8oxoG[69, 67]. They also found that no insertion, extension, or

elongation occurred for the 1,N^6-ethenoadenine, which is understandable given the severe conformational different 1,N^6-ethenoadenine possesses from A alone[70].

Lee's group found in 2009 that pol δ inserts, extends and elongates past both O6meG, 8oxoG, and AP sites, with the highest extension observed past 8oxoG[71].

Guengerich and his group investigated how pol δ encountered O6 alkylated lesions on Guanine including the insertion kinetics of pol δ when it binds to different lesioned templates. Lesions used were O6meG, O6benzylG (O6BzG) , and O6-[4-oxo-4-(3-pyridyl)butyl]G (O6pobG). What they found was that pol δ could bind and replicate past both O6meG and O6BzG, but not O6pobG. They also examined the kinetics of one base incorporation by pol δ and they found that insertion of C opposite G was significantly faster than insertion of C opposite O6meG and O6BzG. Kinetic rate constants, k_{cat}, for incorporation of C were 0.0096 +/- 0.0001 s^{-1} for G, .021 +/- 0.001 s^{-1} for O6meG, and 0.016 +/- 0.001 s^{-1} for O6BzG[72].

A common theme with recent literature is that it challenges the belief that pol δ cannot replicate past DNA lesions. All these papers have deliberately shown that pol δ can replicate past numerous DNA lesions. These novel discoveries raise questions to the method of DDT, how it works, and how involved DDT is in the process of pol δ navigating past DNA lesions. It remains unclear how DDT is activated in human cells and exactly what role it plays regarding insertion, extension, and elongation past a lesion. Furthermore, most of this literature only shows that pol δ is capable of inserting dNTPs across lesions. However, this was done at the expense of abnormal experimental conditions of high concentrations of dNTPs, pol δ, and extremely long reaction times. The experimental system was manipulated to maximize the possibility of insertion where DNA was essentially always bound by pol δ, and dNTPs were flooding the reaction so that as soon as the pol δ-DNA duplex formed the correct conformation for dNTP insertion, a dNTP was

nearby and ready. Although significant, this does not predict what happens in vivo. As stated before, pol δ concentrations in vivo are less than that of DNA, this indicates pol δ does not have unlimited chances incorporate the correct dNTP. Also, pol δ does not have minutes to replicate short sequences of DNA. For these reasons it remains unclear whether a progressing pol δ holoenzyme is capable of inserting a dNTP across a lesion, extending past the lesion, and or elongating the remaining DNA template well at physiological cellular conditions.

To assess pol δ capabilities of lesion bypass at a physiological level, we designed primer extension experiments of a progressing pol δ holoenzyme encountering a DNA lesion using physiological pH, ionic strength, and dNTP concentrations in our reaction mixture. Our analyses will provide single nucleotide resolution via gel electrophoresis, single hit encounters of pol δ holoenzymes with DNA lesions. To do this, all lesions were placed greater than or equal to 9 nucleotides downstream from a P/T junction, and pol δ concentrations will be much lower than DNA concentrations. By doing this, any pol δ holoenzymes in the reaction that dissociate from DNA will likely rebind to an unextended DNA and not one that has been replicated before and pol δ will be progressing along the DNA strand at full kinetic power. Furthermore, reaction times are designed so that the vast majority of DNA in the reaction mixture remains unextended further increasing the likelihood of single hit encounters a pol δ holoenzyme.

Chapter 5

Experimental Methods

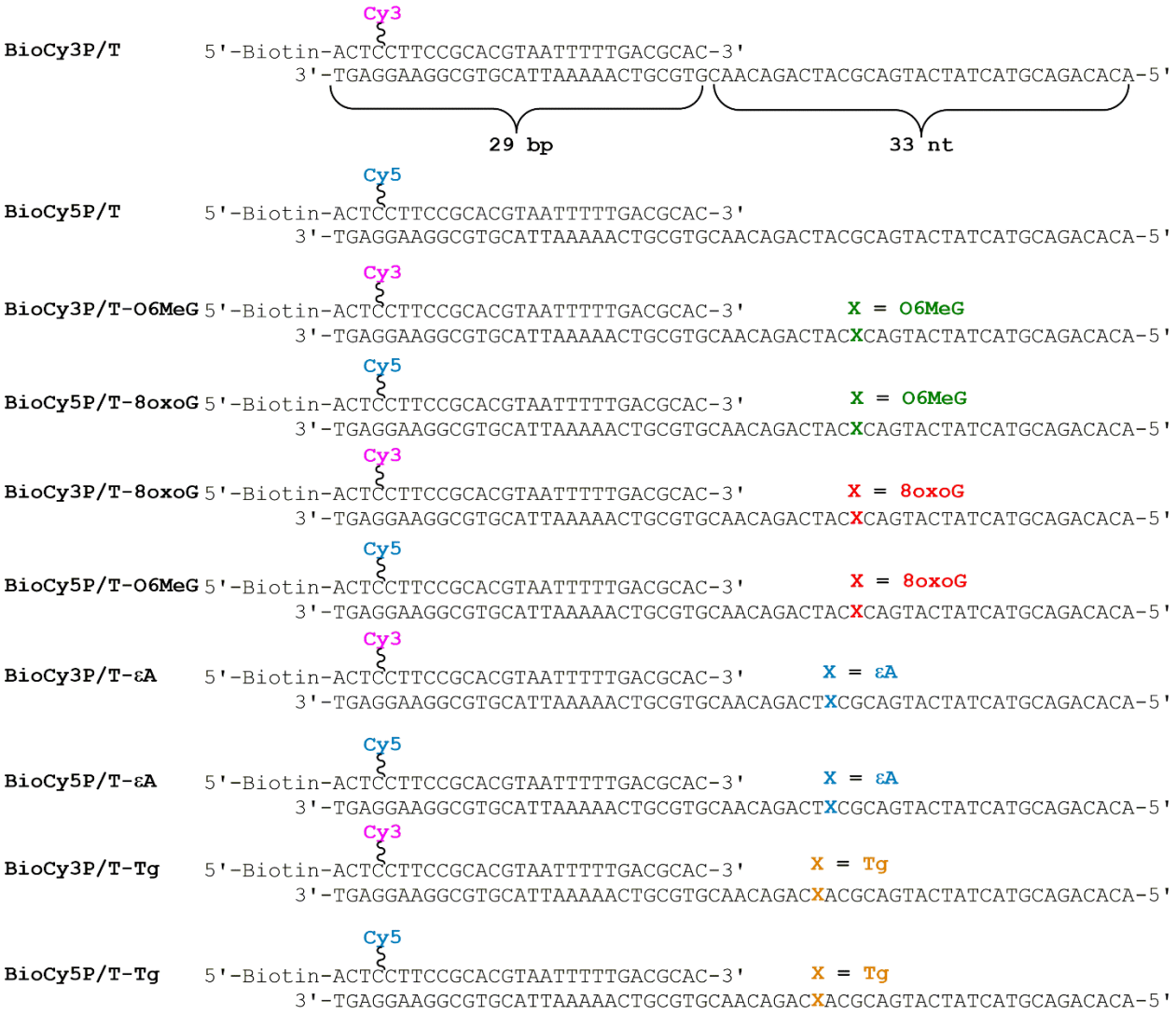

Figure 6. All DNA Primer/Template oligonucleotides used in this study. All primers used were 29 nt, and all templates were 62 nt in length[59].

P/T length allows for a single stranded region large enough for 1 RPA molecule, which is found to take up 29 nt of ssDNA[73-75]. For all experiments, Biotin was attached to Neutravidin to prevent PCNA from sliding off the dsDNA 5' end.

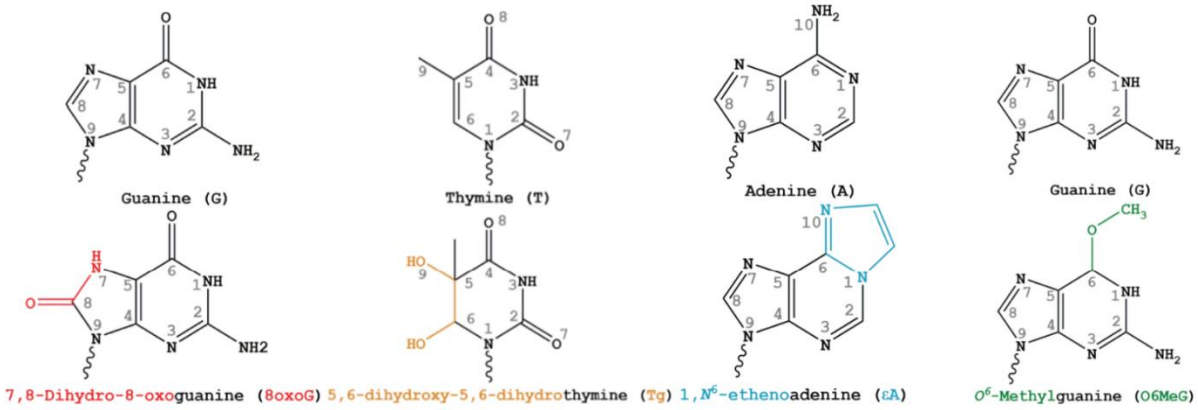

Figure 7. Native nucleotides (top) and their respective lesions (bottom) used for experimentation.

DNA Purification

Temp-62, EthenoA, 8-Oxo-G, and O^{6}-MeG DNA oligonucleotides (oligo) are each 62 nucleotides in length and are synthesized by Integrated DNA Technologies (Coralville, IA) or Bio-Synthesis (Lewisville, TX). Each oligo was then purified separately on an 8% denaturing polyacrylamide-urea gel. Oligonucleotide band of interest was then extracted from the gel via razor extraction. Extracted gel containing DNA was forced through a 10mL needle-less syringe into a 50mL falcon tube, crushing the gel into fragments. Filtered TE Buffer (includes 10mM Tris-HCl pH 8.0 and 1mM EDTA) was added to the falcon tube doubling the total volume for future experimental purposes. Solution was vortexed, flash frozen by liquid N_2, and rocked overnight at room temperature. Contents were removed via Steriflip vacuum filtration (Millipore, Billerica, MA). Filtered contents were then desalted via a C18 reverse phase column (Sep-pak, Waters, Milford, MA). Column was prepped with washes of water and TE Buffer. DNA solution was loaded onto column and moved back and forth via syringes until A_{260} of TE buffer being washed through column was lowest. Column was then washed again with TE Buffer, and DNA was eluted with 30% acetonitrile. Final DNA absorbances were calculated via A_{260} on Nanodrop UV-Vis spectrum and concentrations were calculated via extinction coefficients of each Oligo.

Recombinant Human Proteins

Human RPA, Cy5-PCNA, RFC and pol δ (both exo- and WT) were purified in lab as previously described[76,77]. RPA concentration was found via FRET-based activity assay as described previously[78].

FRET-based assays

Forster Resonance Energy Transfer (FRET) was used to test whether PCNA was loaded onto the Primer/Template DNA at the same rate for Temp-62 and the lesioned substrates. This was accomplished by using a Cy3 labeled Primer and Cy5 labeled PCNA. The closer the two dyes, the higher the FRET signal given off which is indicative of proper loading and is a method widely utilized to test the proximity of proteins and other substrates. Experiments were performed at room temperature (23+/- 2 ^{o}C). Reaction mixtures consisted of 133.34 uL total volume comprised of 25 mm HEPES, pH 7.5, 10 mm $Mg(OAc)_2$, 125 mm KOAc) 1 mm DTT, and the final ionic strength was adjusted to physiological (200 mm) by the addition of appropriate amounts of KOAc. The cuvette used for experimentation was a 16.100F-Q-10/Z15 sub-micro fluorometer cells (Starna Cells) and the instrument used was a Horiba Scientific Duetta-Bio fluorescence/absorbance spectrometer. Our final reaction mixtures contained 110 nM of a Bio-Cy3P/T DNA, 440 nM neutravidin and 1 mM ATP that was pre-incubated with RPA (330 nM heterotrimer). Next, Cy5-PCNA (100 nM homotrimer) was added. Finally, RFC (100 nM heteropentamer) was added, the resultant solution was mixed via rapid pipetting. E_{FRET} was measured starting around 10 seconds after addition of RFC, and time courses were correctly adjusted to reflect this. Reaction mixtures are excited at 514nm, and emission intensities are recorded at 563nm for Cy3 (I_{563}) and 665nm for Cy5 (I_{665}). Band pass slit widths are set to 5nm

and time points are taken every .17s for 300s. For each time point a FRET signal is calculated as E_{FRET} where $E_{FRET}= I_{665}/ (I_{563}+I_{665})$.

Primer Extension Assays

Primer extension assays were performed in lab at 25 ^{o}C with physiological conditions. Proteins were placed in liquid Nitrogen for storage during assays, while ATP and DTT were kept in ice before use. Assays for each oligo were carried out in triplicate, and a separate assay buffer was used for each trial. Replication buffer was 1 x and consisted of 1mM DTT, 1mM ATP, and an adjusted ionic strength of 230mM via appropriate KOAc addition for each reaction buffer. To set up the assay, Bio-Cy-5-P29-C primer was annealed to each oligonucleotide template. Annealing was carried out by creating equal concentrations of primer and a given template and adding 10% reaction volume of a 10X annealing buffer. Reaction was warmed at 95 ^{o}C, and allowed to cool to room temperature. Annealing's and reaction mixtures were kept out of light as much as possible. Regarding the assay itself, the following substrates were added, and the reaction mixture was vortexed and spun down after each mixture. First 250nM Cy5-labeled P/T DNA was incubated with 1uM neutravidin. Replication Protein A (RPA) (750nM) was added next and allowed to incubate for 5 minutes. PCNA (250 nM) was added next. Then 1mM ATP, and 250nM Replication Factor C (RFC) are added and incubated for 5 minutes as determined from the RFC-catalyzed loading assays. Next, dNTPs are added consisting of 46uM dATP, 9.7uM dGTP, 48uM dCTP, and 67uM dTTP. Initiation of primer extension stems from the addition of pol δ (8.8nM for Wild Type (WT), and 35nM for exo-). The concentrations of dNTP's used are consistent with the physiological concentrations of purines and pyrimidines found by Traut[79]. Once initiated, aliquots were removed at variable timepoints from the reaction mixture and quenched with 62.5 mM EDTA, pH 8.0, 2 M Urea, 50% formamide and 0.01% (wt/vol) tracking

dyes in a 1:1 aliquot: quench ratio. Aliquots were taken typically until 60 seconds for exonuclease deficient assays and less than 120 seconds for wild type assays. Aliquots were then heated at 95 ^{o}C for 5 minutes, then immediately placed on ice for 5 minutes. Aliquots were then separated on a 16% denaturing poly-acrylamide urea gel. Gel images were taken on a Typhoon Model 9410 gel imager. Gel images were then quantified based on their fluorescence band intensities using Image Quant (GE Healthcare). A concentration was assigned to each band on the primer extension products by taking the total intensities for a single lane, then dividing each band by the total intensity and multiplying that by the concentration of P/T DNA used in the assay, which was 250 nM. In any lane, the probability of incorporation, P_i, for each dNTP incorporation step, i, is determined by taking all of the fluorescence intensity from band $i + 1$ to the products and dividing that number by the total fluorescence intensity from band i to the products. This probability gives the probability of inserting a dNTP across either a native nucleotide or a lesion and represented by the symbol, P_i. Insertion efficiencies for each DNA lesion were determined by dividing the insertion probability for a lesion by the insertion probability for a native nucleotide at the same position, and then multiplying that decimal by 100%. Referencing figure 6, all lesioned templates contain the same nucleotide sequence as the native Template-62 sequence, and any lesion is replaced by its native, unmodified nucleotide in the Template-62 oligonucleotide. Extension probability refers to the probability of dNTP incorporation 1nt downstream of a DNA lesion or a native nucleotide and is equal to P_{i+1}. Extension efficiency is determined by dividing the extension probability of a lesioned template by the extension probability of a corresponding native nucleotide in the same position and then multiplying by 100%. Bypass probability was determined for any specific nucleotide by multiplying the probability of insertion across that nucleotide, $P_{i,}$ by the probability of insertion

for the next nucleotide, P_{i+1}. Bypass efficiency for each lesion was determined by dividing the bypass probability for a lesion by the bypass probability for its native nucleotide and multiplying that value by 100%. The fraction of pol δ that dissociates around a lesion can be quantified by taking the band intensity at a specific nucleotide, i, and dividing it by the band intensities at all following nucleotides from i+1 to the end of the sequence. All experiments were run at least three separate times using separate reaction mixtures for each replicate and timepoints were only used for analysis if the reaction completeness was under 20% as determined by intensity of products divided by total intensity of a lane.

Chapter 6

Results and Discussion

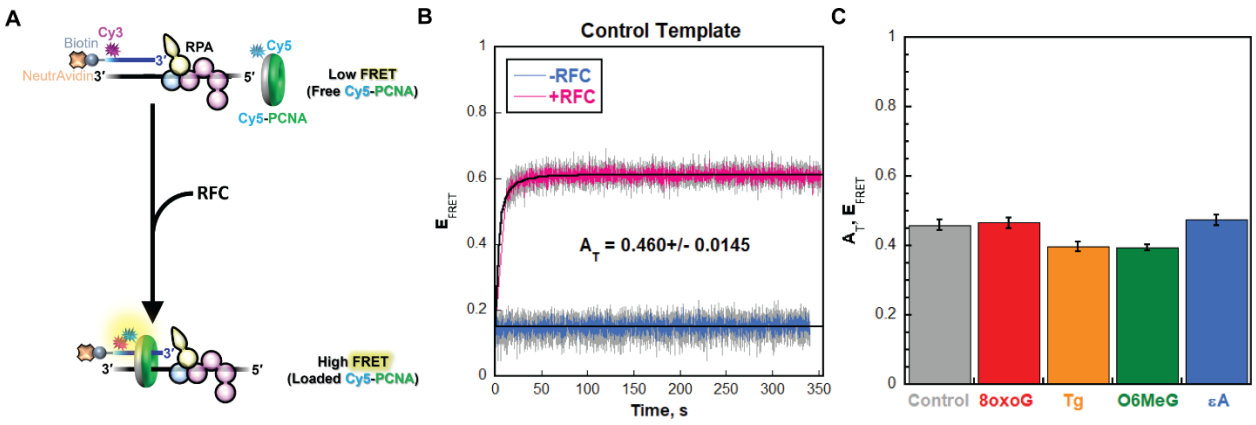

Figure 8. DNA lesions do not influence RFC-catalyzed loading of PCNA onto P/T DNA[59].(A) General schematic of the RFC catalyzed PCNA loading assay. (B) FRET signals observed over 300 seconds in the absence and presence of RFC for BioCy3P/T DNA (control). (C) A_T values for BioCy3P/T, BioCy3P/T-8oxoG, BioCy3P/T-Tg, BioCy3P/T-O6MeG, and BioCy3P/T-εA DNA substrates[59].

FRET was used to determine if lesioned templates containing 8oxoG, Tg, O6MeG, or eA had any effect on the RFC catalyzed loading of PCNA onto P/T DNA substrate. All experiments were performed in triplicate and involve sequential additions of BioCy3-29/62mer P/T DNA, Neutravidin, RPA, Cy5-PCNA, and RFC. BioCy3 primer is the FRET donor, and Cy5-PCNA is the FRET acceptor. The Cy3 label on the primer is located 4 nt from the 5' terminus of the primer, and the Cy5 label on PCNA is located on the back face of PCNA, shown in grey in figure 8. The front face of PCNA is facing forward and is what ultimately binds to pol δ during replication. Using this setup, correct loading of PCNA onto P/T DNA will increase the FRET signal seen between the Cy3 and Cy5 dyes. FRET is a measure of distance, where the closer in distance the dyes are, the higher the signal produced. Seen in figure 8a, the correct loading of

PCNA onto a P/T DNA substrate will produce a high FRET signal, E_{FRET}. Looking at part B, E_{FRET} was plotted as a function of time for 300 seconds to determine the change in E_{FRET} after the addition of RFC to the reaction mixture. Each point is the average of at least three replicates including standard errors. We see that E_{FRET} was very low and constant in the absence of RFC indicating PCNA is not loaded onto P/T DNA. When RFC was added, E_{FRET} increased substantially with time and the FRET traces shown in figure 8b can be fit to a double exponential rise where the amplitude, A_T, between the two phases represents the change in E_{FRET} in the presence of RFC catalyzed loading of Cy5-PCNA onto BioCy3P/T DNA. Each lesioned P/T substrate was tested in this exact manor and their A_T values were determined use the same methods as for the control. We found that BioCy3P/T, BioCy3P/T-8oxoG, BioCy3P/T-Tg, BioCy3P/T-O6MeG, and BioCy3P/T-εA DNA substrates all demonstrated identical loading of PCNA onto their templates by RFC and that the lesions have no affect on the loading of PCNA onto their substrates[59]. For the control, BioCy3P/T substrate, A_T values are consistent with other literature[31,77,78,80-85].

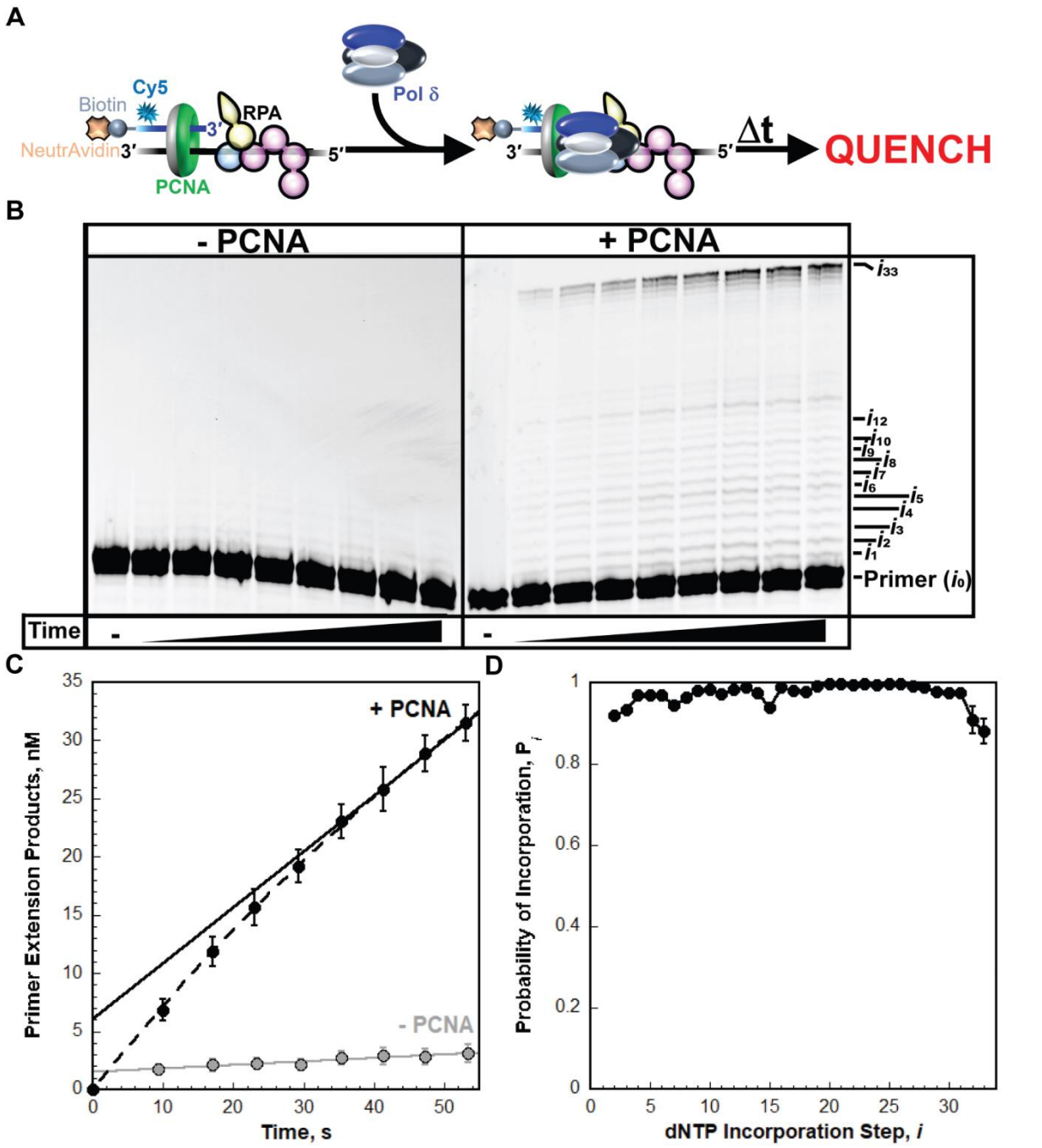

Figure 9. Overview of replication of an undamaged template by pol δ holoenzymes[59]. (A) General schematic of primer extension assays used for both control and lesion containing templates. (B) 16% denaturing sequencing gel showing primer extension products of the control template in the presence (right) and absence (left) of PCNA. (C) Primer Extension Products as a function of time in both the presence and absence of PCNA. (D) Probability of Insertion, P_i, values for primer extension products in the presence of PCNA.

In figure 9a we see a general schematic representation of the replication assays performed to determine pol δ capabilities of replicating control and lesioned P/T DNA templates. This schematic is essentially a visual representation of the primer extension assay described in the experimental methods of this paper. Figure 9b shows an image of a 16% denaturing sequencing gel used as a control experiment without any lesions. Shown on the left side is primer extension products in the absence of PCNA, and on the right side is primer extension products in the presence of PCNA. On the right side of part b, i represents which dNTP incorporation step corresponds to which band. For example, i_1 represents the first dNTP incorporation step while i_{33} represents the final dNTP incorporation step. There are 34 total bands seen, one for the unextend substrates and 33 for each possible primer extension product. Here, the presence of PCNA significantly improves the function of pol δ. On the left-hand side, hardly any replication has occurred. On the right side, significant primer extension products have accumulated over the same time scales. In the absence of PCNA, only 1.249 +/- 0.314% of the primer was extended over 60 seconds. On the right side, 12.60 +/- 0.61% of the primer was extended in the presence of PCNA[59]. The significance of this finding is that under reproducible timescales, we can confirm that all DNA synthesis past the 5th nucleotide must have stemmed from a pol δ holoenzyme and not pol δ itself. The increased synthesis of pol δ in the presence of PCNA agrees with experiments performed by Hedglin and Johansson[84,86]. Figure 9c shows primer extension products vs time in the presence and absence of PCNA. Burst kinetics are observed in the presence of PCNA while the linear primer extension rates are observed in the absence of PCNA. Initial velocity of the linear phase can be determined from the slope given in nM/s. The linear phase data points can be fit to a linear regression to determine the amplitude of the burst phase. The amplitude of the burst phase is equal to the Y intercept found from the linear

regression and has units of nM. Figure 9d shows the probability of incorporation, P_i, also referred to as the processivity, of pol δ holoenzymes replicating a control P/T DNA template. P_i values seen in figure 9d are from the primer extension assay in the presence of PCNA. Under standard conditions we see that the pol δ holoenzyme is very processive and has no difficulty replicating an undamaged DNA template. All processivity values were above 0.8, with most of them near 1.0 which agrees with previous literature values[84,85]. None of our values had a processivity of 1.0, indicating some fraction of pol δ dissociates after each dNTP incorporation step[59]. This is also consistent with findings from other literature sources[84,85]. This experiment, and all other primer extension experiments in this paper are defined as single hit. What this means is that all primer extension products result from a single pass of a pol δ holoenzyme replicating a substrate. To do this, reaction completion is kept under 20% for data analysis. This ensures that any pol δ that may dissociate from a DNA strand will most likely rebind to a fresh, unreplicated DNA strand. This essentially negates the chance that pol δ rebinds after a lesion, and promotes the idea that all lesions are replicated, or attempted to be replicated, through one attempt only. Given the results from figures 8 and 9, we can confirm that our lesioned substrates will not be replicated by pol δ alone, and that PCNA will be properly loaded onto P/T DNA and the pol δ holoenzyme will have a running start at the lesion where each lesion sits at least 9 nt downstream from the P/T junction where replication is initiated.

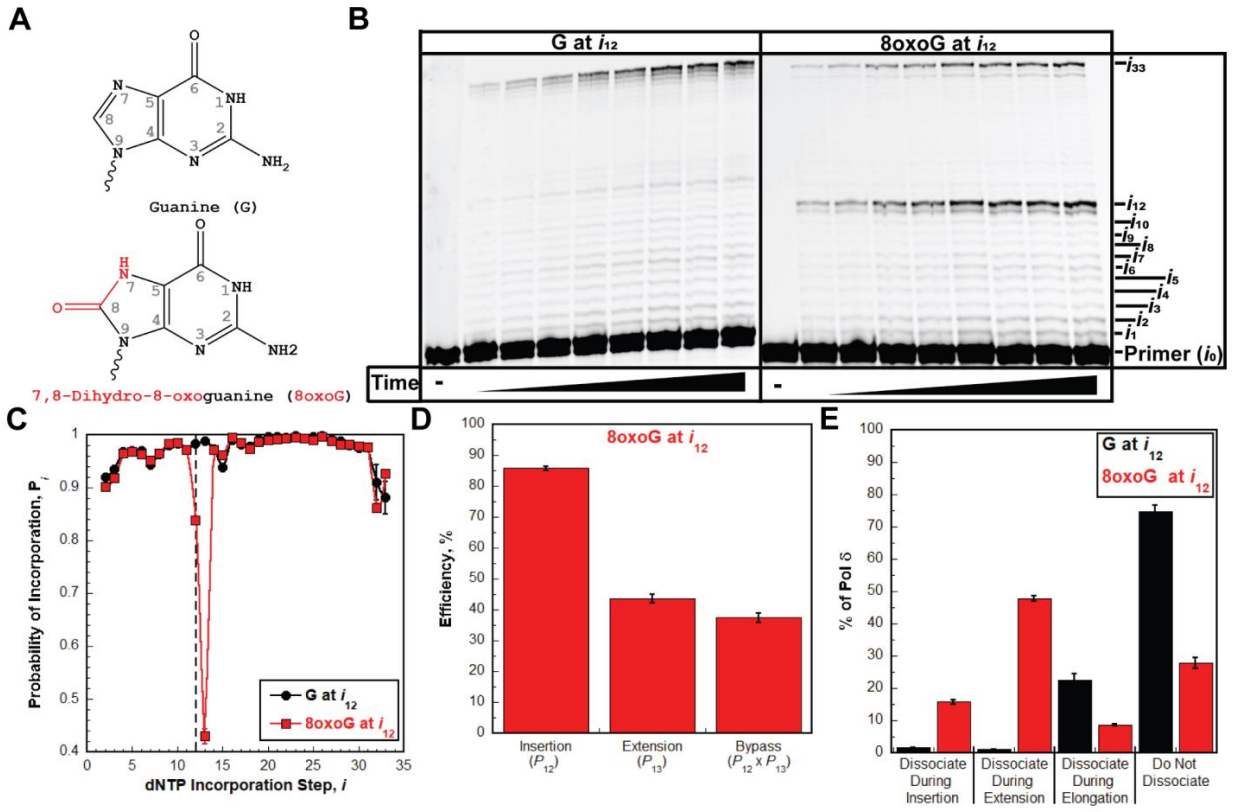

Figure 10. Results from primer extension assay where pol δ holoenzymes encountered 8oxoG lesions. (A) Structures of native Guanine and the oxidative lesion 7,8-Dihydro-8-oxoguanine (8oxoG) used in this assay. (B) 16% denaturing sequencing gel displaying primer extension products for Bio-Cy5-P/T ('G at i12')(left) and Bio-Cy5-P/T-8oxoG ('8oxoG at i12')(right). (C) Probability of incorporation as a function of dNTP incorporation step, i, for both G and 8oxoG. (D) Efficiency of insertion, extension, and bypass relating 8oxoG to native G at position i_{12}. Percent of pol δ dissociation around an 8oxoG lesion (red) or native Guanine (black) during primer extension by a pol δ holoenzyme[59]. Our primer extension assay involved a progressing pol δ holoenzyme encountering an 8oxoG lesion at the i_{12} position downstream of the P/T junction. This can be seen as the 13th band counting from the bottom in figure 10B (right). 8oxoG results in the addition of an oxo group on the 8th carbon of Guanine, a purine nucleotide. Along with the addition of the oxo group, the nitrogen at position 7 becomes reduced. This assay utilized both templates Bio-Cy5-P/T and Bio-Cy5-P/T-8oxoG to test probabilities and efficiencies in the presence and absence of a lesion. All other nucleotides in these primer template sequences are identical.

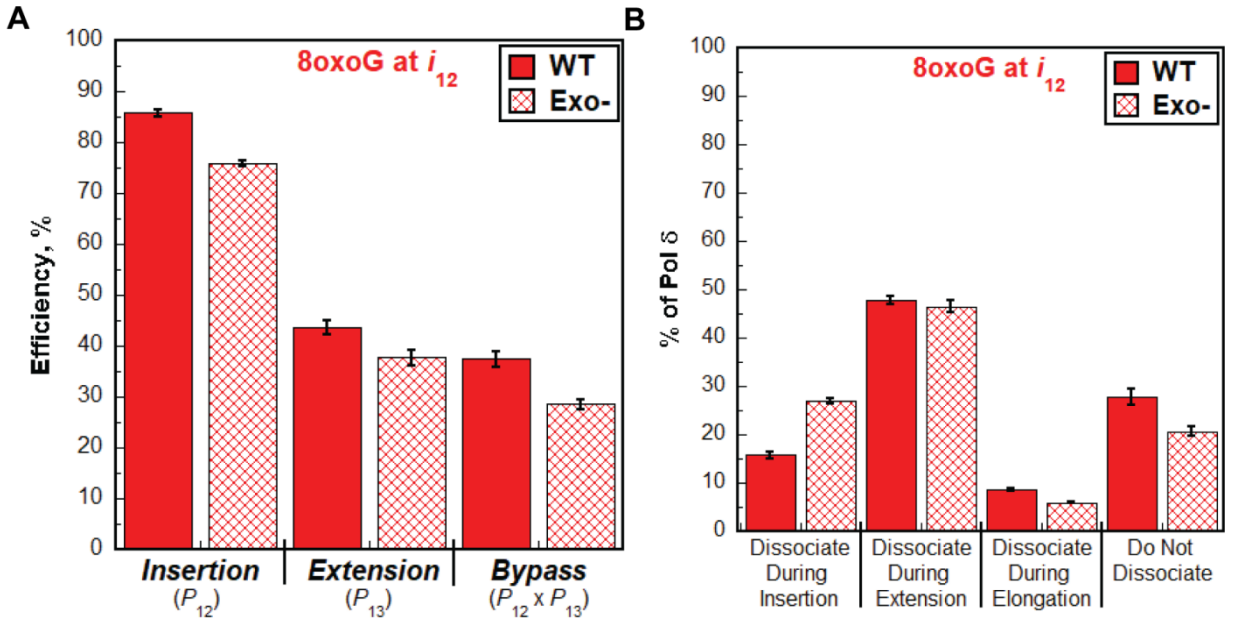

Figure 11. Characterizing the encounters of the pol δ holoenzyme with an 8oxoG lesion in the presence or absence of exonuclease activity. (A) Efficiency percentages of pol δ holoenzyme (exo- and WT) inserting, extending, and bypassing the 8oxoG lesion. (B) Dissociation of pol δ (exo- and WT) around the 8oxoG lesion (i_{12} position) split into dissociation during insertion, extension, elongation, or no dissociation[59].

Effect of 8oxoG lesions on pol δ holoenzymes

7,8-Dihydro-8-oxoguanine (8oxoG) is a DNA lesion that arises from the result of oxidative damage to cellular DNA[54]. Oxidative damage can arise both endogenously and exogenously via the exposure of DNA with reactive oxygen species (ROS)[48]. Starting with figure 10b, we clearly see that full length products are seen at the i_{33} position indicating replication has completed and the human pol δ holoenzyme was able to replicate a 33 nt ssDNA with the presence of an 8oxoG lesion on it. Along with this, human pol δ was able to incorporate stable dNTPs before, across, and after an 8oxoG lesion, agreeing with previous literature sources using various experimental methods[67,69,71]. Moving to part C of figure 10, we observe that the P_i values for the insertion of dNTPs by pol δ holoenzymes in the Bio-Cy5-P/T templates and Bio-Cy5-P/T-8oxoG templates are essentially identical including up to the 11th, i_{11}, nucleotide insertion step. This indicates the

presence of a structural deformity in the DNA template, in this case an 8oxoG lesion, is not noticed beforehand by a progressing pol δ holoenzyme. At the lesion nucleotide position, i_{12}, we see that pol δ holoenzymes incorporate a dNTP across the lesion with a P_i value of 0.84 but are less productive at extending lesions with a P_i value of 0.43 at the nucleotide position directly after the lesion, i_{13}. All progressing pol δ holoenzymes that were able to extend the 8oxoG lesion were then able to elongate the remaining ssDNA with the same probability of insertion as the native Bio-Cy5-P/T template, shown in figure 10C. Pol δ holoenzymes are 85.7 +/- 0.6% efficient at inserting a dNTP across the 8oxoG lesion. Further along these lines, pol δ holoenzymes are 43.7 +/- 1.5% efficient at inserting a dNTP one nucleotide past the lesion. Pol δ holoenzymes are 37.5 +/- 1.5% efficient at bypassing the lesion[59]. As mentioned before, from the i_{14} to i_{33} positions, the probabilities of incorporation for pol δ holoenzymes are the same for both the control and lesioned templates. Figure 10 parts C-D tell us that the presence of 8oxoG primarily effects dNTP incorporation across the lesion and extending past the lesion by 1 nt (insertion and extension events). To further asses the replicative abilities of pol δ holoenzymes on the 8oxoG lesion, the dissociation of pol δ distributed around the 8oxoG lesion at the i_{12} position of the Bio-Cy5-P/T-8oxoG template was compared side by side to the pol δ dissociation distribution about the i_{12} position on the Bio-Cy5-P/T template. What we saw was consistent with the data in figures 10B-D. In figure 10E, for the native, Bio-Cy5-P/T template, of the pol δ that reached the i_{12} position, 74.7 +/- 2% of it did not dissociate during the rest of replication from i_{12} to i_{33}. Of the pol δ holoenzymes that reach the 8oxoG lesion on the damaged Bio-Cy5-P/T-8oxoG lesioned templated, only 27.8 +/- 1.6% makes it the entire way through replication without dissociation, a significantly smaller value than its control counterpart[59]. Of the pol δ replicating the control sequence, the majority of dissociation events had to do with the elongation

steps, not the i_{12} or i_{13} positions. Regarding the pol δ replicating the 8oxoG lesions, 47.8 +/- 1.6% of pol δ dissociated during extension, and 15.8 +/- 0.6% dissociated during insertion. This agrees that pol δ has an easier time inserting a dNTP across the 8oxoG lesion, but a harder time extending 1nt past the lesion.

We also assessed the whether the 3'→5' proofreading activity of pol δ had an effect on the ability of pol δ replicating 8oxoG lesions. To do this, we performed primer extension assays using either WT pol δ or exo- pol δ. Due to the single hit design of the assay, any proofreading that occurs will be intrinsic meaning pol δ does not dissociate and then rebind to proofread. Inhibition of exonuclease activity may increase the proficiency of pol δ holoenzymes inserting, extending, and or elongating past 8oxoG lesions. On the other hand, if the presence of exonuclease activities is beneficial to the incorporation of dNTPs across and past 8oxoG lesions, then inhibiting this function on pol δ will decrease the capabilities of pol δ holoenzymes to replicate past 8oxoG lesions. Whichever effect proofreading has, we have manipulated the experiment to ensure that it is of intrinsic nature during a single binding encounter. We found that the WT pol δ holoenzyme was more efficient at inserting across, extending, and bypassing 8oxoG lesions than exo- pol δ holoenzymes. Seen in figure 11A, inhibiting exonuclease activity decreased the bypass efficiency by 8.91 +/- 1.84%, the insertion efficiency by 9.88 +/- 0.91%, and the extension efficiency by 6.01 +/- 2.07%[59]. What we see in figure 11B is that dissociation events during extension and elongation are for the most part unchanged. However, the decrease in the percentage of exo- pol δ that does not dissociate is made up for by an increase in the percentage of pol δ that dissociates during insertion. Overall, progressing pol δ holoenzymes incorporate dNTPs during insertion, extension, and elongation on 8oxoG lesions, and pol δ holoenzymes are not affected by 8oxoG lesions from i_1-i_{11} and i_{14}-i_{33} at physiological conditions.

Effect of Tg lesions on pol δ holoenzymes

5,6-dihydroxy-5,6-dihydrothymine, also called Thymine Glycol (Tg), is another predominant DNA lesion resulting from oxidative damage[48]. Thymine itself is the most susceptible nucleobase to oxidation with 10-20% of genome damage stemming from ionizing radiation. Estimates have shown at least 400 Tg residues arise in every cell every day, and Tg lesions pose a significant challenge for replication[87]. In figure 12B, we can see that less primer extension products exist for the Tg lesioned template (right) compared to the control template with no lesion (left). However, a substantial amount of completed products have formed showing qualitatively that pol δ holoenzymes can insert, extend, and elongate past Tg lesions by stable incorporation of dNTPs. In figure 12C, we see that probability of insertion, P_i, values are the same for both Bio-Cy5-P/T and Bio-Cy5-P/T-Tg templates from insertion steps i_1-i_8 and from i_{12}-i_{33} telling us that pol δ holoenzymes are likely not affected travelling up to the lesion until the lesion itself, and likely are not affected once they are 3 or more nt downstream of the lesion. This is possibly due to the conformation change Tg lesions can exhibit on nucleotides downstream of them. Tg lesions possess 5R Tg cis-trans epimerization where the methyl group seen on carbon 5 in figure 12 assumes an axial or equatorial position. In the axial position, it extends far enough to disrupt neighboring nucleotides' position possibly interfering with down strand replication past the lesion[87].Also observed in figure 12C, P_i for Tg lesion is significantly smaller than that of

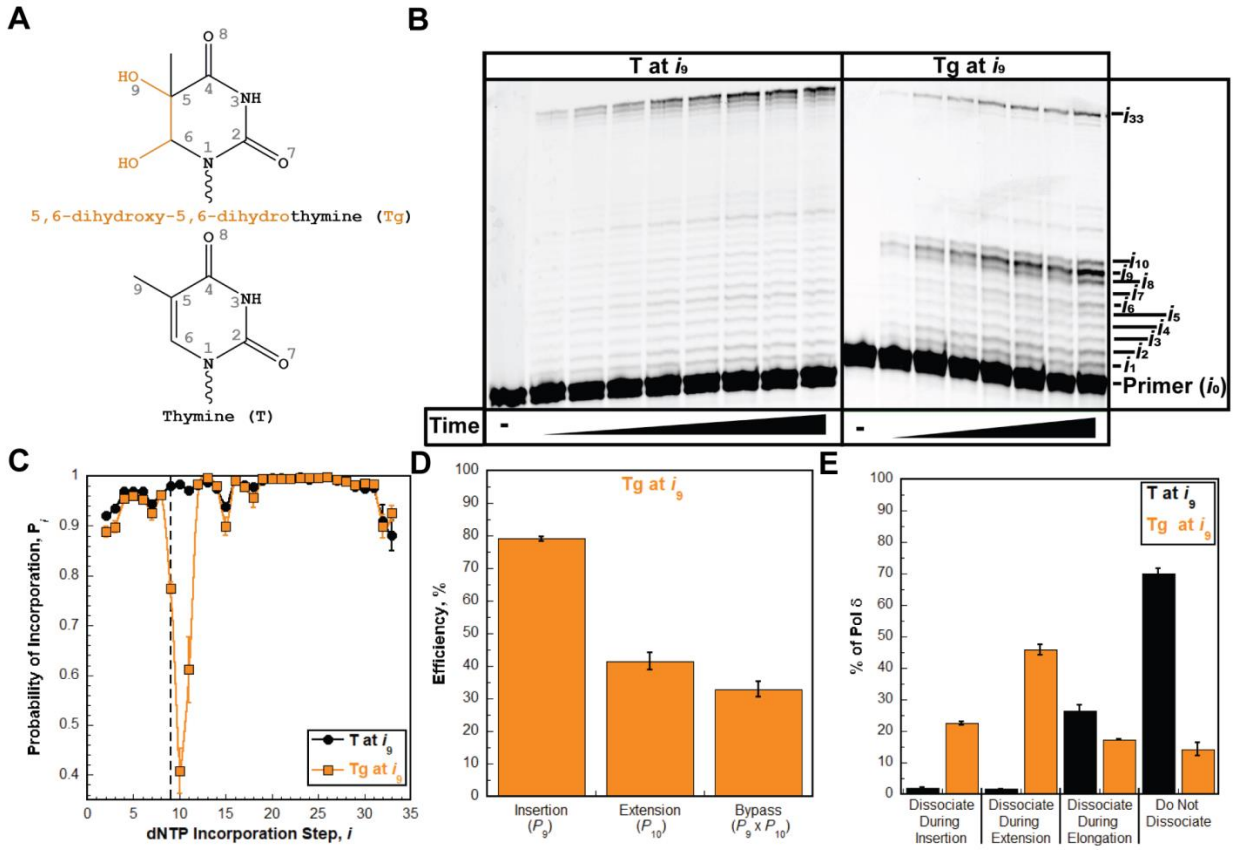

Figure 12. Results from primer extension assay where pol δ holoenzymes encountered 5,6-dihydroxy-5,6-dihydrothymine lesions. (A) Structures of native Thymine and the oxidative lesion 5,6-dihydroxy-5,6-dihydrothymine (Tg) used in this assay. (B) 16% denaturing sequencing gel displaying primer extension products for Bio-Cy5-P/T ('T at i_9') (left) and the Bio-Cy5-P/T-Tg ('Tg at i_9') (right). (C) Probability of incorporation as a function of dNTP incorporation step, i, for both T and Tg. (D) Efficiency of insertion, extension, and bypass relating Tg to native T at position i_9. Percent of pol δ dissociation around a Tg lesion (orange) or native Thymine (black) during primer extension by a pol δ holoenzyme[59]. Our primer extension assay involved a progressing pol δ holoenzyme encountering an Tg lesion at the i_9 position downstream of the P/T junction. This can be seen as the 10th band counting from the bottom in figure 12B (right). Tg results from the addition two hydroxyl groups at the 5th and 6th carbons of the pyrimidine, Thymine. This assay utilized both templates Bio-Cy5-P/T and the Bio-Cy5-P/T-Tg to test probabilities and efficiencies in the presence and absence of a lesion. All other nucleotides in these primer template sequences are identical.

native T for the insertion, extension, and the first elongated nt. We see this more clearly in figure 12D where the insertion efficiency of Tg was 79.1 +/- 0.7%, the extension efficiency was 41.5 +/- 2.7% and the bypass. efficiency were 31.6 +/- 2.3%[59]. Only 31.6 +/- 2.3% of pol δ

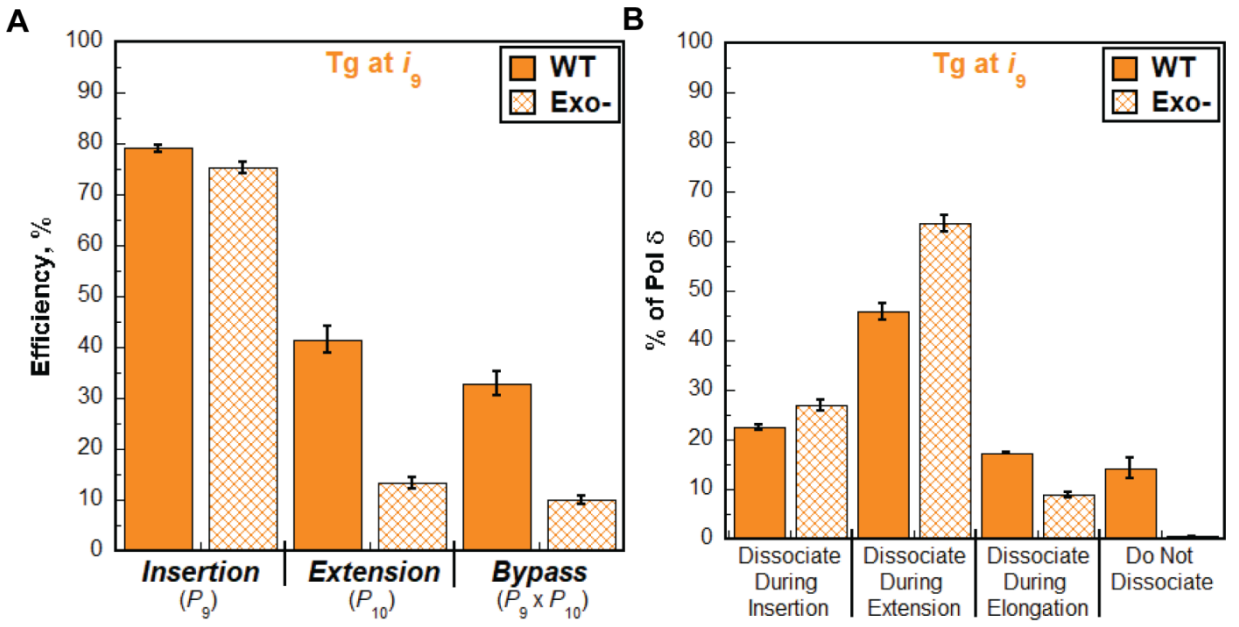

Figure 13. Characterizing the encounters of the pol δ holoenzyme with a Tg lesion in the presence or absence of exonuclease activity. (A) Efficiency percentages of pol δ holoenzyme (exo- and WT) inserting, extending, and bypassing the Tg lesion. (B) Dissociation of pol δ (exo- and WT) around the Tg lesion (i_9 position) split into dissociation during insertion, extension, elongation, or no dissociation[59].

holoenzymes are able to by-pass the lesion (P_9 x P_{10}), which is significantly less than the bypass percentage of native Thymine (96.3 +/- 0.2%[59]. Pol δ holoenzymes are affected by insertion, extension, and the first nucleotide involved in elongation past the Tg lesion. Seen in figure 12E, 22.5 +/- 0.7% of pol δ holoenzymes dissociate during insertion, 45.9 +/- 1.7% of pol δ dissociate during extension, and 17.4 +/- 0.3% dissociate during elongation. Lastly, 14.3 +/- 2.1% of pol δ does not dissociate at all when replicating the Tg lesion[59]. Moving down to figure 13, we compared the insertion, extension, and bypass abilities of progressing pol δ holoenzymes replicating Tg lesions in the presence and absence of exonuclease activity. We first see in figure 13A that the insertion efficiencies are hardly changed between exo- and WT pol δ. As for extension efficiency, exo- pol δ was 28.2 +/- 2.9% less efficient at extending Tg lesions as the WT variant was. Keeping the same trend, exo- pol δ was also 22.9 +/- 2.5% less efficient at Tg

lesion bypass the WT counterpart[59]. Most dissociation events for pol δ have occurred during extension and elongation, with slightly more occurring for exo- than WT. Furthermore, only a small fraction of exo- pol δ did not dissociate from the DNA. All of this indicated exonuclease proficient, WT, pol δ was more efficient at replicating Tg lesions that exo- pol δ. Whether the exonuclease activity is proofreading incorrect dNTPs to promote more efficient extension and elongation, or exonuclease activity is stabilizing correct dNTP incorporation at the extension site remains to be known.

Effect of O6MeG lesions on pol δ holoenzymes

O^6-Methylguanine, or O6MeG, is a common alkylative lesion resulting from endogenous or exogenous alkylating agents. Literature has come closer to the conclusion that *N*-nitroso compounds, such as nitrosamines are potentially carcinogenic in humans, and they are known to produce the O6MeG lesion[89]. One such disease associated with defective repair of O6MeG by the enzyme O^6-methylguanine-DNA methyltransferase is hepatocellular carcinogenesis[90]. The lesioned template, Bio-Cy5-P/T-O6MeG contains the O6MeG at position i_{12}. As we first see in figure 14B, full length products are observed in the primer extension assays using the Bio-Cy5-P/T-O6MeG template which is indicative of progressing pol δ holoenzymes being capable of replicating past O6MeG lesions at physiological conditions. Replication past O6MeG lesions also includes stable incorporation of dNTPs during insertion, extension, and elongation. Seen in figure 14C, insertion steps i_1-i_{11} show almost identical probability of insertion, P_i, values for both the native Bio-Cy5- P/T ('G at i_{12}') and the Bio-Cy5-P/T-O6MeG ('O6MeG at i_{12}') DNA substrates indicating progressing pol δ holoenzymes are most likely not affected by the presence

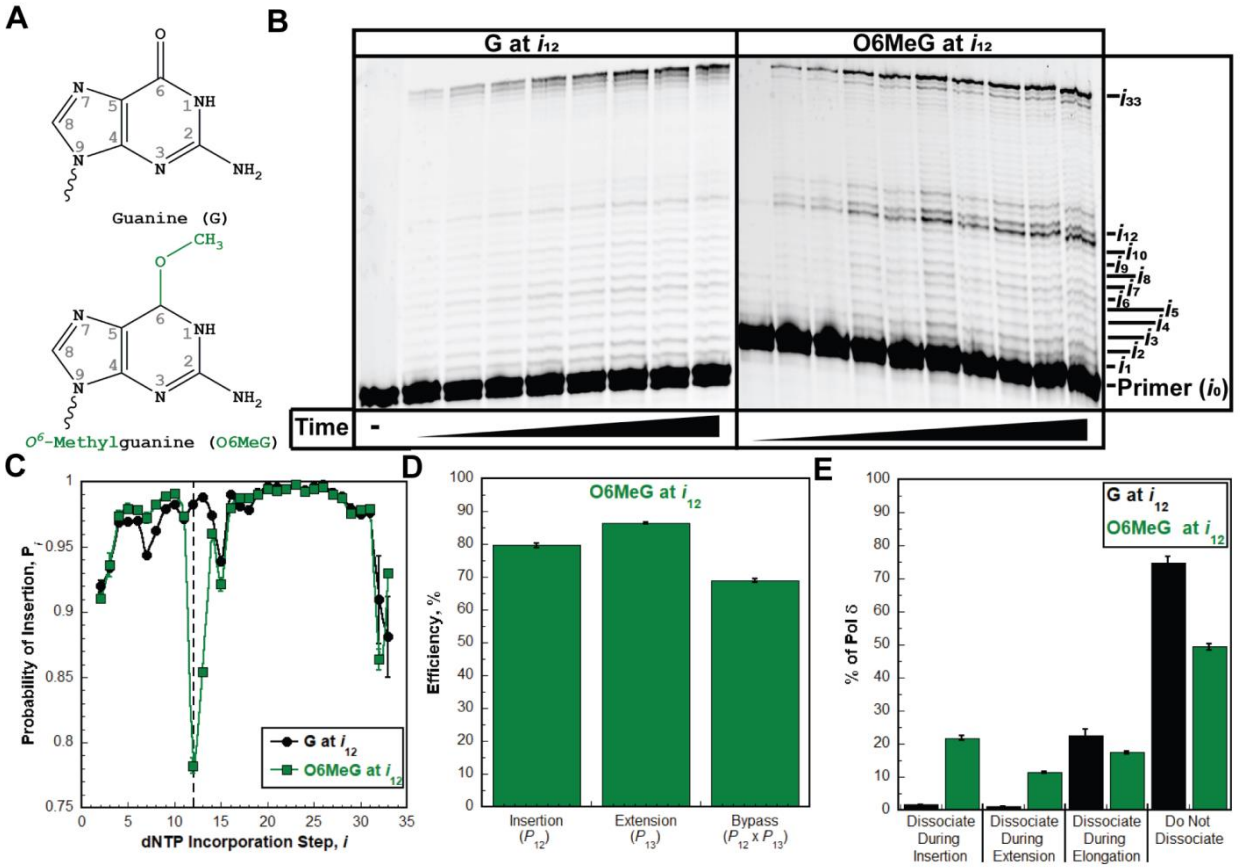

Figure 14. Results from primer extension assay where pol δ holoenzymes encountered O6-Methylguanine lesions. (A) Structures of native Guanine and the methylated lesion O6-Methylguanine (O6MeG) used in this assay. (B) 16% denaturing sequencing gel displaying primer extension products for Bio-Cy5-P/T ('G at i_{12}') (left) and the Bio-Cy5-P/T-O6MeG ('O6MeG at i_{12}') (right). (C) Probability of incorporation as a function of dNTP incorporation step, i, for both G and O6MeG. (D) Efficiency of insertion, extension, and bypass relating O6MeG to native G at position i_{12}. Percent of pol δ dissociation around a O6MeG lesion (green) or native Guanine (black) during primer extension by a pol δ holoenzyme[59]. Our primer extension assay involved a progressing pol δ holoenzyme encountering an O6MeG lesion at the i_{12} position downstream of the P/T junction. This can be seen as the 13th band counting from the bottom in figure 14B (right). O6MeG results in the addition a methyl group on the carbon 6 oxygen in the purine, Guanine. This assay utilized both templates Bio-Cy5-P/T and the Bio-Cy5-P/T-O6MeG to test probabilities and efficiencies in the presence and absence of a lesion. All other nucleotides in these primer template sequences are identical.

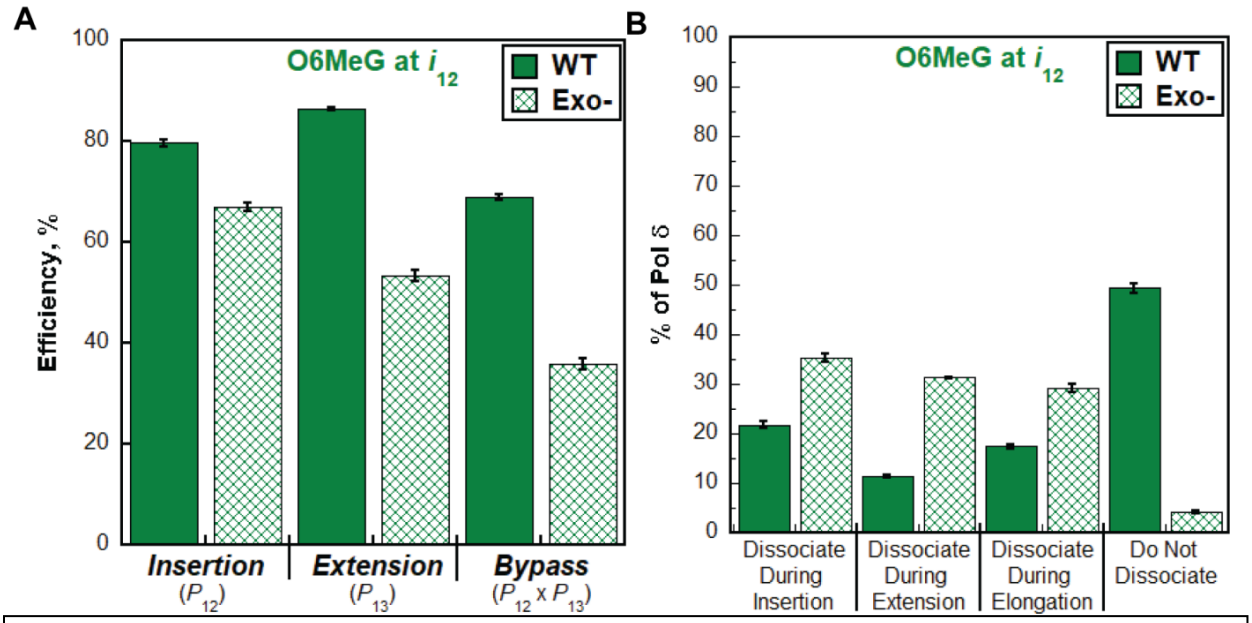

Figure 15. Characterizing the encounters of the pol δ holoenzyme with an O6MeG lesion in the presence or absence of exonuclease activity. (A) Efficiency percentages of pol δ holoenzyme (exo- and WT) inserting, extending, and bypassing the O6MeG lesion. (B) Dissociation of pol δ (exo- and WT) around the O6MeG lesion (i_{12} position) split into dissociation during insertion, extension, elongation, or no dissociation[59].

of the O6MeG lesion on nucleotides before the lesion. Also, dNTP insertion steps i_{14}-i_{33} are very similar for both the native and lesioned templates indicating once two nucleotides past the O6MeG lesion indicating pol δ holoenzymes are likely not affected by the O6MeG lesion in extension of the remaining DNA substrate. As shown in figure 14D, 66.8 +/- 0.6% of progressing pol δ holoenzymes bypass the O6MeG lesion, which is significantly less than that of native G (97.1 +/- 0.1%). These values create a bypass efficiency of 68.8 +/- 0.6%. Insertion efficiency for the O6MeG lesion was 79.6 +/- 0.6%, and the extension efficiency was 86.5 +/- 0.3%[59]. According to figure 14E, 21.8 +/- 0.6% of pol δ dissociates during insertion, 11.4 +/- 0.2% of pol δ holoenzymes dissociated during extension, and 17.5 +/- 0.4% dissociated during elongation. Lastly, to our surprise, pol δ holoenzymes were remarkably efficient in replicating past O6MeG lesions with 49.3 +/- 0.9% of pol δ holoenzyme not dissociating at all during

replication of the lesion. Overall, pol δ holoenzymes were remarkably efficient at incorporating dNTPs across and after the O6MeG alkylative lesion. We then tested whether exonuclease activity of pol δ had any effect on the insertion, extension, elongation, and or bypass of the O6MeG lesion. As with previous lesions, we reconstituted our primer extension assays at physiological conditions and repeated with exonuclease-deficient pol δ exo-. Looking at figure 15A, the WT pol δ shows better efficiency in dNTP insertion, extension, and bypass of the O6MeG lesion. Exo- pol δ exhibited decreased bypass efficiency by 33 +/- 1.3%, decreased insertion efficiency by 12.6 +/- 1.0%, and decreased insertion efficiency by 33.1 +/- 1.0%[59]. A more telling side to this is observed in figure 15b, where dissociation events by the exo- pol δ is higher in all facets. Dissociation during insertion increased with exo- pol δ from 21.8 +/- 0.6% to 35.4 +/- 0.8%. Dissociation during extension increased from 11.4 +/- 0.2% to 31.3 +/- 0.2%, and dissociation during elongation increased from 17.5 +/- 0.4% to 29.2 +/- 0.8% from WT to exo- pol δ[59]. Results of primer extension assays involving O6MeG lesions show that human WT pol δ can very efficiently replicate past O6MeG lesions in a single hit manner at physiological conditions. This is rather understandable as the O6MeG lesion produces a rather small structural deformity to native Guanine. Also, unlike Tg, the O6MeG lesion did not have any effect on dNTP incorporation two nucleotides downstream of the lesion indicating the lesion itself does not likely affect DNA structure or pol δ more than 1 nucleotide downstream of it. This can be observed with the P_i values shown in figure 14C.

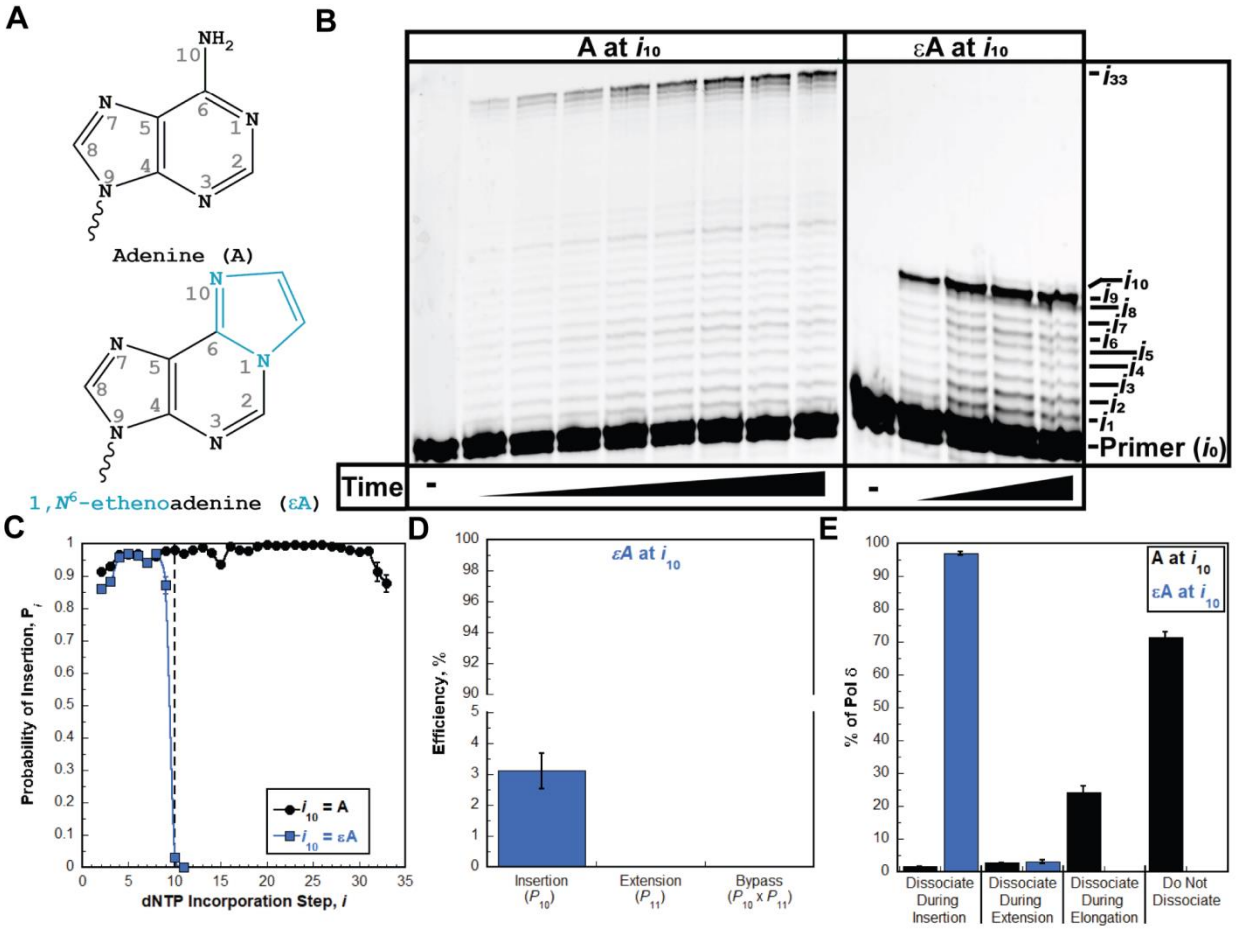

Figure 16. Results from primer extension assay where pol δ holoenzymes encountered 1, N^6-ethenoadenine lesions. (A) Structures of native Adenine and the methylated lesion 1, N^6-ethenoadenine (εA) used in this assay. (B) 16% denaturing sequencing gel displaying primer extension products for native Bio-Cy5-P/T ('A at i_{10}') (left) and the Bio-Cy5-P/T-εA ('εA at i_{10}') (right) DNA templates. (C) Probability of incorporation as a function of dNTP incorporation step, i, for both A and εA. (D) Efficiency of insertion, extension, and bypass relating εA to native A at position i_{10}. Percent of pol δ dissociation around an εA lesion (Blue) or native Adenine (black) during primer extension by a pol δ holoenzyme[59]. Our primer extension assay involved a progressing pol δ holoenzyme encountering an eA lesion at the i_{10} position downstream of the P/T junction. This can be seen as the 11^{th} band counting from the bottom in figure 16B (right). εA lesions results in the addition of two carbons that attach to nitrogen 1 and 10 forming a five membered exocyclic ring. This assay utilized both templates Bio-Cy5-P/T and Bio-Cy5-P/T-εA to test probabilities and efficiencies in the presence and absence of a lesion. All other nucleotides in these primer template sequences are identical.

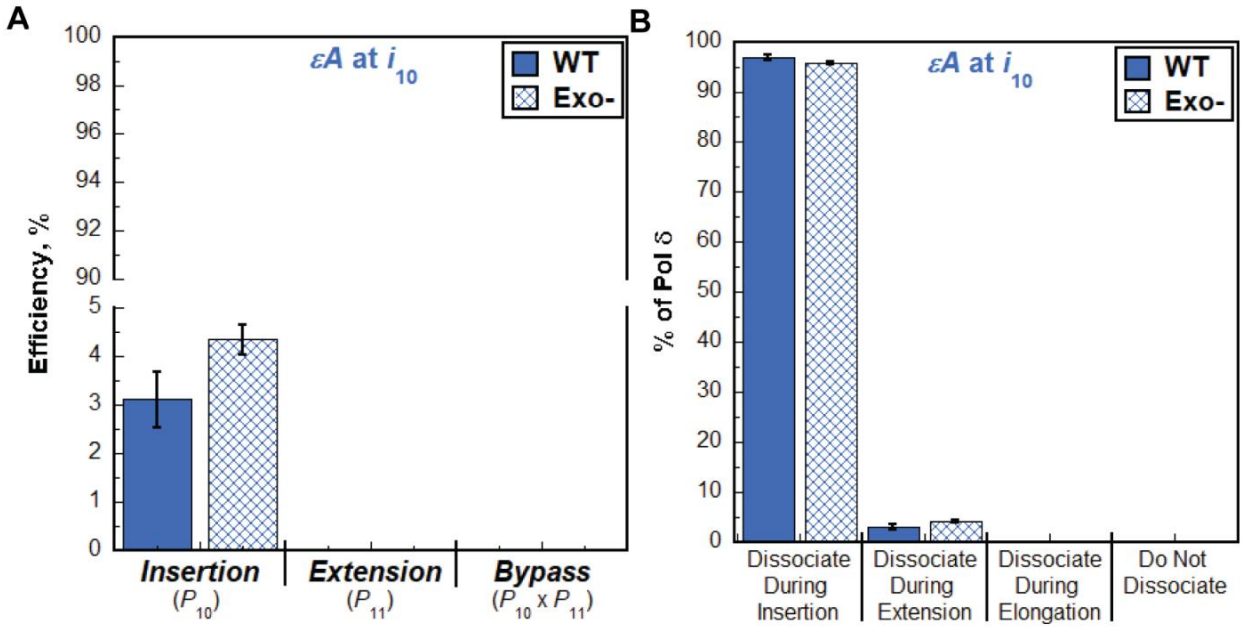

Figure 17. Characterizing the encounters of the pol δ holoenzyme with an εA lesion in the presence or absence of exonuclease activity. (A) Efficiency percentages of pol δ holoenzyme (exo- and WT) inserting, extending, and bypassing the εA lesion. (B) Dissociation of pol δ (exo- and WT) around the εA lesion (i_{10} position) split into dissociation during insertion, extension, elongation, or no dissociation[59].

Effect of eA lesions on pol δ holoenzymes

1, N^6-ethenoadenine (εA) is a common alkylative DNA lesion that results from the exposure of DNA to vinyl chloride or lipid peroxidation and is a potential carcinogen in formation of lung cancer[88]. Shown in figure 16B, the εA lesion is located at the i_{10} position downstream of the P/T junction. Hardly any pol δ was able to insert a dNTP across the lesion. Extension past the lesion was not observed. This clearly shows that presence of the εA lesion inhibits the insertion and extension so much that pol δ dissociates from the DNA in one of those steps. Another important note, shown more clearly in figure 16C, is that probability of insertion, P_i, for the 9th insertion step is slightly less for the Bio-Cy5-P/T-εA template compared to the native e Bio-Cy5-P/T-template. Insertion steps i_1-i_8 are very similar for both the native and eA templates indicating dNTP insertion by pol δ holoenzymes is not affected until the insertion step before the eA lesion.

Looking at figure 16D, only 3.06 +/- 0.56% of progressing DNA holoenzymes can incorporate a dNTP across the εA lesion. Due to the insertion percentage on native A (98.3 +/- 0.1%), the insertion efficiency of pol δ inserting across an εA lesion is 3.11 +/- 0.57%[59]. Also seen in figure 16D is that pol δ was not able to extend past the εA lesion, and subsequently was not able to bypass the lesion either. Knowing this, it is clear that all pol δ holoenzyme dissociation occurred during the insertion and extension steps with the insertion step being responsible for the majority of dissociation (96.9 +/- 0.6%) and the remaining pol δ dissociated during extension. Like our previous lesions, we then tested whether the proofreading activity of pol δ had any effect on replicating an εA lesion. What was saw was that inactivating exonuclease activity of pol δ had no effect on any of the aforementioned qualitative observations or the measured variables These results show that εA imposes a severe problem to progressing pol δ holoenzymes severely impacting their ability to insert dNTPs both before and after the εA lesion and is in agreement with previous literature findings involving similar studies[70].

Looking below at figure 18A, we see the efficiency percentages of pol δ inserting, extending, and bypassing each lesion. It is first clear to note that of the lesions studied, εA imposed the greatest difficulty to pol δ. 8oxoG, Tg, and O6MeG all had relatively similar insertion efficiencies, and pol δ was most successful at replicating the O6MeG lesion with it having the highest extension and bypass efficiencies of all lesions. In figure 18B we see a similar story where essentially all pol δ dissociated during the insertion step on εA. Also, as mentioned before eA was the only lesion to cause significant dissociation before the lesion. 8oxoG and Tg

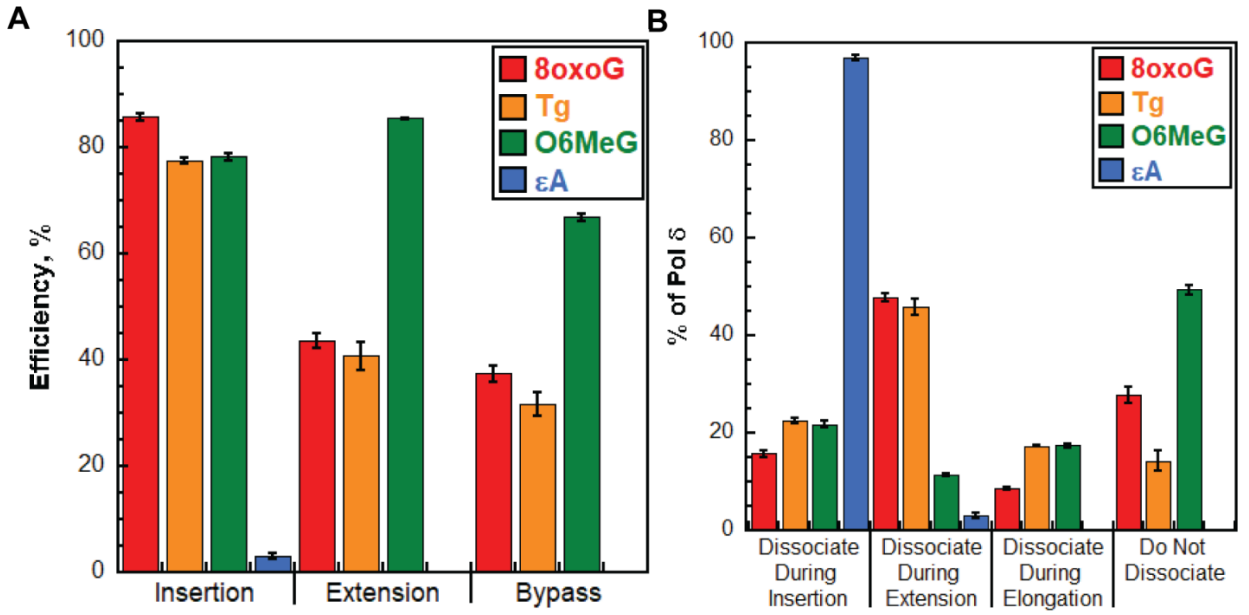

Figure 18. Lesion bypass capabilities of progressing pol δ holoenzymes during initial encounters. This data represents a culmination of figures 17, 15, 13, and 11. (A) Efficiencies of progressing WT pol δ holoenzymes in their ability to insert, extend, and bypass DNA lesions used in this study. (B) Dissociation percentages of progressing pol δ holoenzymes distributed around the lesion at insertion, extension, elongation, and no dissociation[59].

templates have very similar dissociation distributions of pol δ around their respective lesions, with slightly more pol δ not dissociating during replication of the 8oxoG lesion. Reiterated in this figure is that pol δ was most successful in replicating O6MeG lesions.

Chapter 8

Conclusion

This study involved the reconstitution of lagging strand DNA synthesis by human pol δ holoenzymes at human physiological conditions including, pH, ionic strength, and dNTP concentration. We aimed to quantify the interaction of pol δ holoenzymes with various DNA lesions located downstream (at least 9 nt) of a P/T junction in a single hit manner. By doing this, pol δ holoenzymes would have a "running start" at the lesion where they would be fully tracking and binding to DNA would not affect the lesion replicated. The single hit manner entails the use of high DNA concentration to low pol δ concentration so that if pol δ dissociated from the DNA, rebinding to a fresh DNA would be much more likely than a previously replicated strand. Results of this study show that pol δ can insert dNTPs across three lesions; 8oxoG, O6MeG, and Tg with greater than 80% efficiency, and if pol δ can not replicate fully past the lesion, dissociation events are distributed around the DNA lesion and not just during insertion across the lesion[59]. Human pol δ holoenzymes show proficiency at inserting dNTPs across 8oxoG lesions with an insertion efficiency of 85.7 +/- 0.6%. Also, the WT variant of pol δ showed increased insertion efficiency by 9.88 +/- 0.91% indicating pol δ holoenzymes replicate a large amount of 8oxoG lesions without the help of DDT pathways such as TLS. Based on previous quantitative analyses, we estimate that correct C is incorporated across the 8oxoG lesion 50-63% of the time, and incorrect A is incorporated across 8oxoG 21-34% of the time [54,59,67,69]. These findings indicate when a C is incorporated by pol δ opposite 8oxoG, DDT pathways are likely only involved to finish replication upon stalling of the pol δ holoenzyme. However, when an A is incorporated, several issues arise as an incorrect nucleotide is incorporated, and pol δ is likely stalling around

the lesion. The incorrect dAMP must be excised before the following round of replication, or it will become a permanent part of our genome resulting in a mutation.

Like 8oxoG, progressing human pol δ holoenzymes are very efficient at inserting dNTPs across Tg lesions with an insertion efficiency of 79.1 +/- 0.7%. Also like 8oxoG, proofreading proficient WT pol δ increases insertion efficiency by 3.73 +/- 1.32% showing a substantial amount of Tg lesions are faithfully replicated by pol δ holoenzymes in their initial encounter of the lesion rather than a DDT pathway as previously believed[59]. Extension efficiency of Tg lesions was found to be 41.5 +/- 2.7% which is less than the insertion efficiency for Tg. DDT would be most active during the extension step, as that is where the majority of pol δ dissociates during replication of Tg. Our understanding is that studies on the replication of Tg lesions by pol δ holoenzymes have yet to be reported, and that this is the first of its nature. Previous studies have investigated the lesion bypass capabilities of pol α, a primer inserting polymerase that works in tandem with pol δ and pol ε to lay down the first set of nucleotides involved in DNA synthesis[2,3]. It was found that pol α predominantly inserts dAMP across Tg lesions[62].
Pol δ holoenzymes are very efficient at replicating O6MeG lesions with an insertion efficiency of 79.6 +/- 0.6%. Also, proofreading proficient pol δ increases insertion efficiency by 12.6 +/- 1.0% showing once again that O6MeG lesions can and are replicated initially by progressing pol δ holoenzymes without the contributions from DDT. Successful extension of the O6MeG lesion by pol δ agrees with previous literature sources, albeit they were using different reaction conditions[70, 71]. Pol δ holoenzymes were more efficient at extending O6MeG lesions that 8oxoG and Tg with an experimental extension efficiency found to be 86.5 +/- 2.5% telling us that 85.4 +/- 0.2% of progressing pol δ holoenzymes that can insert dNTPs across O6MeG will go on to extend the lesion as well. Proofreading proficient pol δ was also found to contribute 33.1 +/-

1.0% to the extension efficiency. Collectively, this data tells us that O6MeG lesions are largely replicated by human pol δ itself without the help of DDT pathways.

Unlike the previous three lesions, pol δ has a hard time inserting dNTPs across εA lesions with an insertion efficiency of 3.11 +/- 0.57. Moreover, pol δ holoenzymes show zero extension or elongation past the εA lesion, and proofreading does not help with any of these steps. The severity of the εA lesion requires the use of DDT pathways such as TLS to properly replicate

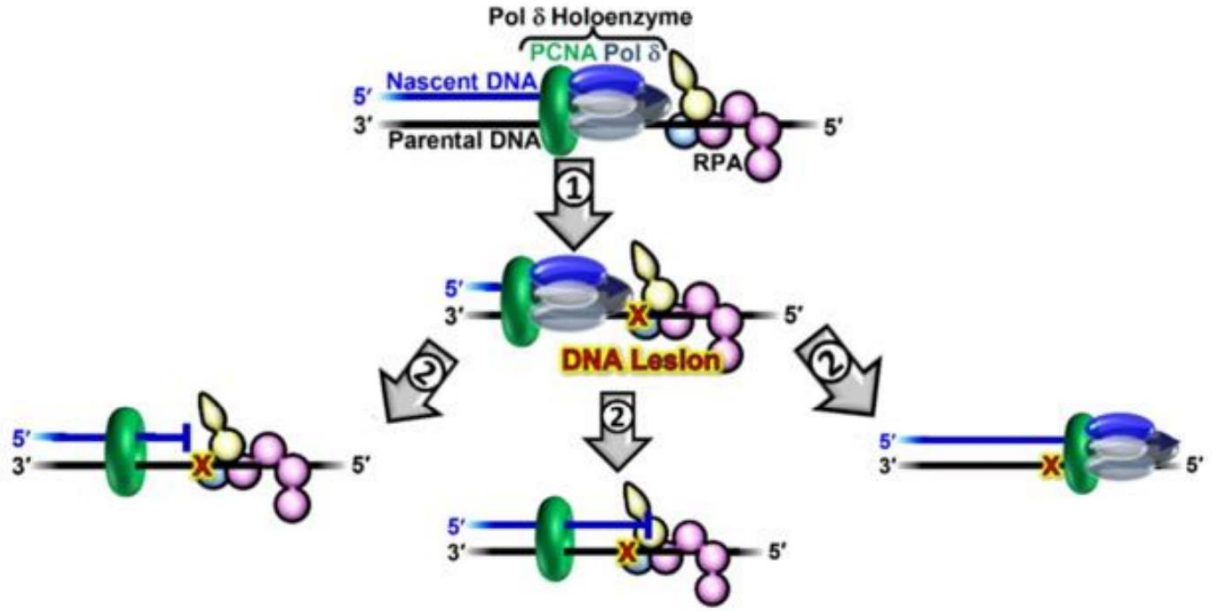

Figure 19. Possible outcomes when progressing pol δ holoenzymes encounter a DNA lesion. On the left side we see dissociation of the pol δ holoenzyme at the insertion step. In the middle we see dissociation during the extension or elongation steps. On the right side we observe a successful bypass of the lesion by pol δ holoenzymes.

past the it which agrees with previous literature[63].

Figure 19 does an excellent job describing the routes that can happen when a progressing pol δ holoenzyme encounters a DNA lesion, in this case 8oxoG, Tg, or O6MeG. Pol δ encountering a lesion does not always immediately involve DDT pathways as previously

thought, thus changing the perspective on the involvement in DDT in lagging strand synthesis by pol δ.

REFERENCES

1- Barnum, K. J. & O'Connell, M. J. in *Cell Cycle Control* Vol. 1170 (eds Noguchi, E. & Gadaleta, M. C.), 29–40 (Springer, 2014).

2- Stucki M, Stagliar I, Jonsson ZO, Hu¨bscher U. 2000. Prog. Nucleic Acid Res. Mol. Biol. 65:261–98

3- Hubscher, U., Maga, G. & Spadari, S. Eukaryotic DNA polymerases. *Annu. Rev. Biochem.* **71**, 133–163 (2002).

4- McCulloch, S. D. & Kunkel, T. A. The fidelity of DNA synthesis by eukaryotic replicative and translesion synthesis polymerases. Cell Res. 18, 148–161 (2008).

5- Pursell, Z. F., Isoz, I., Lundstrom, E. B., Johansson, E. & Kunkel, T. A. Yeast DNA polymerase epsilon participates in leading-strand DNA replication. *Science* **317**, 127–130 (2007).

6- Braithwaite DK, Ito J. 1993. Nucleic Acids Res. 21:787–802

7- Byrnes, J.J.; Downey, K.M.; Black, V.; Esserman, L.; So, A.G. Selective Inhibition of the 3′ to 5′ Exonuclease Activity Associated with Mammalian DNA Polymerase δ. In Miami Winter Symposium: Cancer Enzymology; Schultz, J., Ahmad, F., Eds.; Academic Press: Cambridge, MA, USA, 1976; Volume 12, pp. 245–264.

8- Byrnes, J.J.; Downey, K.M.; Black, V.L.; So, A.G. A new mammalian DNA polymerase with 3′ to 5′ exonuclease activity: DNA polymerase δ. Biochemistry 1976, 15, 2817–2823.

9- Byrnes, J.J.; Downey, K.M.; Que, B.G.; Lee, M.Y.; Black, V.L.; So, A.G. Selective inhibition of the 3′ to 5′ exonuclease activity associated with DNA polymerases: A mechanism of mutagenesis. Biochemistry 1977, 16, 3740–3746.

10- Lee, M.Y.; Byrnes, J.J.; Downey, K.M.; So, A.G. Mechanism of inhibition of deoxyribonucleic acid synthesis by 1-beta-D-arabinofuranosyladenosine triphosphate and its potentiation by 6-mercaptopurine ribonucleoside 5′-monophosphate. Biochemistry 1980, 19, 215–219.

11- Lee, M.Y.; Tan, C.K.; So, A.G.; Downey, K.M. Purification of deoxyribonucleic acid polymerase δ from calf thymus: Partial characterization of physical properties. Biochemistry 1980, 19, 2096–2101.

12- Lee, M.Y.; Tan, C.K.; Downey, K.M.; So, A.G. Structural and functional properties of calf thymus DNA polymerase δ. Prog. Nucleic Acid Res. Mol. Biol. 1981, 26, 83–96.

13- Lee, M.Y.; Tan, C.K.; Downey, K.M.; So, A.G. Further studies on calf thymus DNA polymerase δ purified to homogeneity by a new procedure. Biochemistry 1984, 23, 1906–1913.

14- Lee, M.Y.; Toomey, N.L.; Wright, G.E. Differential inhibition of human placental DNA polymerases δ and α by BuPdGTP and BuAdATP. Nucleic Acids Res. 1985, 13, 8623–8630.

15- Lee, M.Y.; Toomey, N.L. Human placental DNA polymerase δ: Identification of a 170-kilodalton polypeptide by activity staining and immunoblotting. Biochemistry 1987, 26, 1076–1085.
16- Lee, M.Y. Isolation of multiple forms of DNA polymerase δ: Evidence of proteolytic modification during isolation. Biochemistry 1988, 27, 5188–5193.
17- Lee, M.Y.; Alejandro, R.; Toomey, N.L. Immunochemical studies of DNA polymerase δ: Relationships with DNA polymerase α. Arch. Biochem. Biophys. 1989, 272, 1–9.
18- Lee, M.Y.; Jiang, Y.Q.; Zhang, S.J.; Toomey, N.L. Characterization of human DNA polymerase δ and its immunochemical relationships with DNA polymerase α and epsilon. J. Biol. Chem. 1991, 266, 2423–2429.
19- Zhang, J.; Chung, D.W.; Tan, C.K.; Downey, K.M.; Davie, E.W.; So, A.G. Primary structure of the catalytic subunit of calf thymus DNA polymerase δ: Sequence similarities with other DNA polymerases. Biochemistry 1991, 30, 11742–11750.
20- Hao, H.; Jiang, Y.; Zhang, S.J.; Zhang, P.; Zeng, R.X.; Lee, M.Y. Structural and functional relationships of human DNA polymerases. Chromosoma 1992, 102, S121–S127.
21- Yang, C.L.; Chang, L.S.; Zhang, P.; Hao, H.; Zhu, L.; Toomey, N.L.; Lee, M.Y. Molecular cloning of the cDNA for the catalytic subunit of human DNA polymerase δ. Nucleic Acids Res. 1992, 20, 735–745.
22- Lee,M., Wang,X., Zhang,S., Zhang,Z. and Lee,E.Y.C. (2017) Regulation and modulation of human DNA polymerase delta activity and function. Genes (Basel), 8, 190.
23- Hedglin,M., Pandey,B. and Benkovic,S.J. (2016) Stability of the human polymerase delta holoenzyme and its implications in lagging strand DNA synthesis. Proc. Natl. Acad. Sci. U.S.A., 113, E1777–E1786.
24- Wang Y,Zhang Q,Chen H,Li X,Mai W,Chen K,Zhang S,Lee EY,Lee MY,Zhou Y. 2011b. P50, the small subunit of DNA polymerase delta, is required for mediation of the interaction of polymerase delta subassemblies with PCNA. PLoS One 6: e27092.
25- Zhou Y,Meng X,Zhang S,Lee EY,Lee MY. 2012b. Characterization of human DNA polymerase delta and its subassemblies reconstituted by expression in the multibac system. PLoS One 7: e39156.
26- Podust VN,Chang LS,Ott R,Dianov GL,Fanning E. 2002. Reconstitution of human DNA polymerase delta using recombinant baculoviruses: The p12 subunit potentiates DNA polymerizing activity of the four-subunit enzyme. J Biol Chem 277: 3894–3901.
27- Franklin MC,Wang J,Steitz TA. 2001. Structure of the replicating complex of a pol alpha family DNA polymerase. Cell 105: 657– 667.

28- Swan MK,Johnson RE,Prakash L,Prakash S,Aggarwal AK. 2009. Structural basis of high-fidelity DNA synthesis by yeast DNA polymerase delta. Nat Struct Mol Biol 16: 979– 986.
29- Hedglin,M., Kumar,R. and Benkovic,S.J. (2013) Replication clamps and clamp loaders. Cold Spring Harb. Perspect. Biol., 5, a010165.
30- Ason B, Bertram JG, Hingorani MM, Beechem JM, O'Donnell M, Goodman MF, Bloom LB 2000. A model for Escherichia coli DNA polymerase III holoenzyme assembly at primer/template ends. DNA triggers a change in binding specificity of the γ complex clamp loader. J Biol Chem 275: 3006–3015
31- Li, M., Larsen, L. and Hedglin, M. (2020) Rad6/Rad18 Competes with DNA Polymerases eta and delta for PCNA Encircling DNA. *Biochemistry*.
32- Wold MS. 1997. Replication protein A: a heterotrimeric, single-stranded DNA-binding protein required for eukaryotic DNA metabolism. Annu Rev Biochem 66: 61– 92.
33- Oakley GG, Patrick SM. 2010. Replication protein A: directing traffic at the intersection of replication and repair. Front Biosci 15: 883– 900.
34- Wold MS, Kelly T. 1988. Proc. Natl. Acad. Sci. USA 85:2523–27
35- Fairman MP, Stillman B1988. EMBO J. 7:1211–18
36- Coverley D, Laskey RA. 1994. Annu. Rev. Biochem. 63:745–76
37- Leonhardt H, Cardoso MC. 1995. Int. Rev. Cytol. 162B:303–35
38- Newport J, Yan H. 1996. Curr. Opin. Cell Biol. 8:365–68
39-Laskey RA, Madine M. 1996. See Ref. 189, pp. 119–30
40- Campbell CD, Chong JX, Malig M, Ko A, Dumont BL, Han L, Vives L, O'Roak BJ, Sudmant PH, Shendure J, Abney M, Ober C, Eichler EE. Estimating the human mutation rate using autozygosity in a founder population. Nat Genet. 2012 Nov;44(11):1277-81. doi: 10.1038/ng.2418. Epub 2012 Sep 23.
41- Panneerselvam J, Qu D, Houchen C, Bronze M, Chandrakesan P. DCLK1 and DNA Damage Response; IntechOpen, 2020. https://www.researchgate.net/publication/341360174_DCLK1_and_DNA_Damage_Response/citations (accessed Mar 14, 2023).
42- Visconti R, Grieco D. New insights on oxidative stress in cancer. Curr Opin Drug Discov Devel. 2009;12(2):240–245.
43- Reuter S, Gupta SC, Chaturvedi MM, Aggarwal BB. Oxidative stress, inflammation, and cancer: how are they linked? Free Radic Biol Med. 2010;49(11):1603–1616.
44- Perrone S, Lotti F, Geronzi U, Guidoni E, Longini M, Buonocore G. Oxidative Stress in Cancer-Prone Genetic Diseases in Pediatric Age: The Role of Mitochondrial Dysfunction. Oxid Med Cell Longev. 2016;2016:4782426.
45- Bennett JW, Klich M. Mycotoxins. *Clin Microbiol Rev.* 2003;16(3):497–516.
46- Segal AW. How neutrophils kill microbes. Annu Rev Immunol. 2005;23:197–223.

47- Malle E, Furtmuller PG, Sattler W, Obinger C. Myeloperoxidase: a target for new drug development? Br J Pharmacol. 2007;152(6):838–854.
48- Cadet J, Wagner JR. Oxidatively generated base damage to cellular DNA by hydroxyl radical and one-electron oxidants: similarities and differences. *Arch Biochem Biophys.* 2014;557:47–54.
49- Tropp BE. Molecular biology, From gene to protein. 4. Jones & Bartlett Learning; 2011. p. 1100.
50- Imlay JA, Chin SM, Linn S. Toxic DNA damage by hydrogen peroxide through the Fenton reaction in vivo and in vitro. *Science.* 1988;240(4852):640–642.
51- Imlay JA, Chin SM, Linn S. Toxic DNA damage by hydrogen peroxide through the Fenton reaction in vivo and in vitro. Science. 1988;240(4852):640–642.
52- O'Driscoll M, Macpherson P, Xu YZ, Karran P. The cytotoxicity of DNA carboxymethylation and methylation by the model carboxymethylating agent azaserine in human cells. Carcinogenesis. 1999;20(9):1855–1862.
53- Zhao C, Tyndyk M, Eide I, Hemminki K. Endogenous and background DNA adducts by methylating and 2-hydroxyethylating agents. Mutat Res. 1999;424(1–2):117–125.
54- Wang, Yanli & Schlick, Tamar. (2007). Distinct energetics and closing pathways for DNA polymerase β with 8-oxoG template and different incoming nucleotides. BMC structural biology. 7. 7. 10.1186/1472-6807-7-7.
55- Ye N, Holmquist GP, O'Connor TR. Heterogeneous repair of N-methylpurines at the nucleotide level in normal human cells. J Mol Biol. 1998;284(2):269–285.
56- Chatterjee N, Walker GC. Mechanisms of DNA damage, repair and mutagenesis. Environ Mol Mutagen. 2017; 58(5):235-263.
57- Omar Desoukya ND, Zhoub Guangming. Targeted and non-targeted effects of ionizing radiation. Journal of Radiation Research and Applied Sciences. 2015;8(2):247–254.
58- Davies RJ. Royal Irish Academy Medal Lecture. Ultraviolet radiation damage in DNA. Biochem Soc Trans. 1995;23(2):407–418.
59- Rachel L Dannenberg, Joseph A Cardina, Kara G Pytko, Mark Hedglin, Tracking of progressing human DNA polymerase δ holoenzymes reveals distributions of DNA lesion bypass activities. Nucleic Acids Research. 2022;50(17):9893-9908.
60- Harper JW, Elledge SJ. The DNA damage response: ten years after. Mol Cell. 2007;28(5):739–745
61- Krokan HE, Bjoras M. Base excision repair. Cold Spring Harb Perspect Biol. 2013;5(4):a012583.
62- Kusumoto,R., Masutani,C., Iwai,S. and Hanaoka,F. (2002) Translesion synthesis by human DNA polymerase eta across thymine glycol lesions. Biochemistry, 41, 6090–6099.
63- Tolentino,J.H., Burke,T.J., Mukhopadhyay,S., McGregor,W.G. and Basu,A.K. (2008) Inhibition of DNA replication fork progression and mutagenic potential of 1, N6-

ethenoadenine and 8-oxoguanine in human cell extracts. Nucleic Acids Res., 36, 1300–1308.

64- Sale JE. Translesion DNA synthesis and mutagenesis in eukaryotes. Cold Spring Harb Perspect Biol. 2013;5(3):a012708.

65- Hedglin,M. and Benkovic,S.J. (2017) Eukaryotic translesion DNA synthesis on the leading and lagging strands: unique detours around the same obstacle. Chem. Rev., 117, 7857–7877.

66- Hedglin,M. and Benkovic,S.J. (2015) Regulation of rad6/rad18 activity during DNA damage tolerance. Annu. Rev. Biophys., 44, 207–228.

67- Fazlieva,R., Spittle,C.S., Morrissey,D., Hayashi,H., Yan,H. and Matsumoto,Y. (2009) Proofreading exonuclease activity of human DNA polymerase delta and its effects on lesion-bypass DNA synthesis. Nucleic Acids Res., 37, 2854–2866.

68- Narita,T., Tsurimoto,T., Yamamoto,J., Nishihara,K., Ogawa,K., Ohashi,E., Evans,T., Iwai,S., Takeda,S. and Hirota,K. (2010) Human replicative DNA polymerase delta can bypass T-T (6-4) ultraviolet photoproducts on template strands. Genes Cells, 15, 1228–1239.

69- Markkanen,E., Castrec,B., Villani,G. and Hubscher,U. (2012) A switch between DNA polymerases delta and lambda promotes error-free bypass of 8-oxo-G lesions. Proc. Natl. Acad. Sci. U.S.A., 109, 20401–20406.

70- Schmitt,M.W., Matsumoto,Y. and Loeb,L.A. (2009) High fidelity and lesion bypass capability of human DNA polymerase delta. Biochimie, 91, 1163–1172.

71- Meng,X., Zhou,Y., Zhang,S., Lee,E.Y., Frick,D.N. and Lee,M.Y. (2009) DNA damage alters DNA polymerase delta to a form that exhibits increased discrimination against modified template bases and mismatched primers. Nucleic Acids Res., 37, 647–657.

72- Choi,J.Y., Chowdhury,G., Zang,H., Angel,K.C., Vu,C.C., Peterson,L.A. and Guengerich,F.P. (2006) Translesion synthesis across O6-alkylguanine DNA adducts by recombinant human DNA polymerases. J. Biol. Chem., 281, 38244–38256.

73- Kim, C., Paulus, B.F. and Wold, M.S. (1994) Interactions of human replication protein A with oligonucleotides. Biochemistry, 33, 14197-14206.

74- Kim, C., Snyder, R.O. and Wold, M.S. (1992) Binding properties of replication protein A from human and yeast cells. *Mol Cell Biol*, **12**, 3050-3059.

75- Kim, C. and Wold, M.S. (1995) Recombinant human replication protein A binds to polynucleotides with low cooperativity. *Biochemistry*, **34**, 2058-2064.

76- Henricksen,L.A., Umbricht,C.B. and Wold,M.S. (1994) Recombinant replication protein A: expression, complex formation, and functional characterization. J. Biol. Chem., 269, 11121–11132.

77- Hedglin,M., Perumal,S.K., Hu,Z. and Benkovic,S. (2013) Stepwise assembly of the human replicative polymerase holoenzyme. Elife, 2, e00278.

78- Li,M., Sengupta,B., Benkovic,S.J., Lee,T.H. and Hedglin,M. (2020) PCNA monoubiquitination is regulated by diffusion of rad6/rad18 complexes along RPA filaments. Biochemistry, 59, 4694–4702.
79- Traut,T.W. (1994) Physiological concentrations of purines and pyrimidines. Mol. Cell. Biochem., 140, 1–22.
80- Hedglin, M., Aitha, M. and Benkovic, S.J. (2017) Monitoring the Retention of Human Proliferating Cell Nuclear Antigen at Primer/Template Junctions by Proteins That Bind Single-Stranded DNA. *Biochemistry*, **56**, 3415-3421.
81- Hedglin, M., Aitha, M., Pedley, A. and Benkovic, S.J. (2019) Replication protein A dynamically regulates monoubiquitination of proliferating cell nuclear antigen. *J Biol Chem*, **294**, 5157-5168.
82- Hedglin, M. and Benkovic, S.J. (2017) Eukaryotic Translesion DNA Synthesis on the Leading and Lagging Strands: Unique Detours around the Same Obstacle. *Chem Rev*, **117**, 7857-7877.
83- Hedglin, M. and Benkovic, S.J. (2017) Replication Protein A Prohibits Diffusion of the PCNA Sliding Clamp along Single-Stranded DNA. *Biochemistry*, **56**, 1824-1835.
84- Hedglin, M., Pandey, B. and Benkovic, S.J. (2016) Stability of the human polymerase delta holoenzyme and its implications in lagging strand DNA synthesis. *Proc Natl Acad Sci U S A*, **113**, E1777-1786.
85- Hedglin, M., Pandey, B. and Benkovic, S.J. (2016) Characterization of human translesion DNA synthesis across a UV-induced DNA lesion. *Elife*, **5**, e19788, 19781 - 19718.
86- Chilkova,O., Stenlund,P., Isoz,I., Stith,C.M., Grabowski,P., Lundstrom,E.B., Burgers,P.M. and Johansson,E. (2007) The eukaryotic leading and lagging strand DNA polymerases are loaded onto primer-ends via separate mechanisms but have comparable processivity in the presence of PCNA. *Nucleic Acids Res.*, 35, 6588–6597.
87- Dolinnaya,N.G., Kubareva,E.A., Romanova,E.A., Trikin,R.M. and Oretskaya,T.S. (2013) Thymidine glycol: the effect on DNA molecular structure and enzymatic processing. *Biochimie*, 95, 134–147.
88- Rioux, K. L., Delaney, S. (2020) 1,N6-Ethenoadenine: From Molecular to Biological Consequences. *Chem. Res. Toxicol.*, **33**, 2688-2698.
89- Grasso, P. (1987) Experimental liver tumours in animals. *Ballieres Clin Gastroenterol* 1:183–203.
90- Major, G.N., Collier, J. D. (1998) Repair of DNA lesion O6-methylguanine in hepatocellular carcinogenesis. *Journal of Hepato-Biliary-Pancaretic Surg*, 5(4), 355-366.

Joseph Cardina
ACADEMIC VITA

EDUCATION

The Pennsylvania State University | Schreyer Honors College, *Eberly College of Science* **State College, PA**
Bachelor of Science in Chemistry Graduation: May 2023
Minor in Biology

Leadership and Involvement

Penn State Student-Athlete Advisory Board (SAAB) **State College, PA**
Special Events Coordinator *September 2021– May 2022*

- Participated in monthly group meetings
- Connected other student athletes with the surrounding community via outreach
- Collaborated with 11 other executive members to organize various events

Team Representative *September 2020-May 2022*

- Relays information from meetings to 20 team representatives
- Participates in monthly group meetings.

Hedglin Lab **State College, PA**
Undergraduate Research Assistant *June 2021– Present*

- Utilized effective communication and developed lab skills to perform research experiments on DNA damage tolerance through the Benkovic Summer Research Scholarship at Penn State
- Published research in Nucleic Acids Research Journal in September 2022
    - Publication Title: "Tracking of progressing human DNA polymerase δ reveals distributions of DNA lesion bypass activities"
- Presented research at the 2022 Fall Symposium at Penn State University

Bench Mark Program **Lancaster, PA**
Student Mentor *August 2021–Present*

- Actively engaged with and mentored underserved youth ages 14-18
- Deliberated career avenues within sports, college, employment, and entrepreneurship
- Attended student leadership programs held once per week taking advice from successful business owners

INTERCOLLEGIATE ATHLETICS

Penn State University, Division I Men's Track and Field **State College, PA**

- Devoted 20 hours per week to practice, meets, travel, and other responsibilities *August 2019– March 2022*
- Successfully balanced a full honors courseload with a varsity athletic schedule
- Represented over 100 teammates on the Student Athlete Advisory Board
- Gained valuable leadership and team-building experience

WORK EXPERIENCE

New Holland Sales Stables **New Holland, PA**
Barn Operations Assistant *June-Aug 2020,2021*

- Involved with animal sorting, transport, and general barn maintenance
- Facilitated efficient flow of animals on sale days
- Developed disciplinary skills including working long days of up to 20 hours

HONORS AND AWARDS

Track and Field Academic ALL-BIG-TEN Athlete ***2021, 2022***
2021 Benkovic Summer Research Scholar ***Summer 2021***

Dean's List ***6/7 semesters***
Kadtke Family Endowed Grant ***2021, 2022***

ADDITIONAL INFORMATION

Technology: Microsoft Word, Excel, and Power Point
Interests: Sports Medicine, Golf, Football, Track and Field, Fly-Fishing
Involvement: Undergraduate Research Ambassador, Nittany Chemical Society, Fly-Fishing Club